

# Design, Synthesis, and Biological Evaluation of 14-Heteroaromatic-Substituted Naltrexone Derivatives: Pharmacological Profile Switch from Mu Opioid Receptor Selectivity to Mu/Kappa Opioid Receptor Dual Selectivity

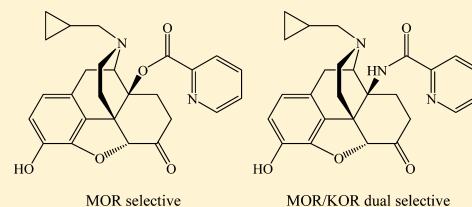
Yunyun Yuan,<sup>†</sup> Saheem A. Zaidi,<sup>†</sup> Orgil Elbegdorj,<sup>†</sup> Lindsey C. K. Aschenbach,<sup>†</sup> Guo Li,<sup>†</sup> David L. Stevens,<sup>‡</sup> Krista L. Scoggins,<sup>‡</sup> William L. Dewey,<sup>‡</sup> Dana E. Selley,<sup>‡</sup> and Yan Zhang<sup>\*,†</sup>

<sup>†</sup>Department of Medicinal Chemistry, Virginia Commonwealth University, 800 East Leigh Street, Richmond, Virginia 23298, United States

<sup>‡</sup>Department of Pharmacology and Toxicology, Virginia Commonwealth University, 410 North 12th Street, Richmond, Virginia 23298, United States

## S Supporting Information

**ABSTRACT:** On the basis of a mu opioid receptor (MOR) homology model and the isosterism concept, three generations of 14-heteroaromatically substituted naltrexone derivatives were designed, synthesized, and evaluated as potential MOR-selective ligands. The first-generation ligands appeared to be MOR-selective, whereas the second and the third generation ones showed MOR/kappa opioid receptor (KOR) dual selectivity. Docking of ligands **2** (MOR selective) and **10** (MOR/KOR dual selective) to the three opioid receptor crystal structures revealed a nonconserved-residue-facilitated hydrogen-bonding network that could be responsible for their distinctive selectivity profiles. The MOR/KOR dual-selective ligand **10** showed no agonism and acted as a potent antagonist in the tail-flick assay. It also produced less severe opioid withdrawal symptoms than naloxone in morphine-dependent mice. In conclusion, ligand **10** may serve as a novel lead compound to develop MOR/KOR dual-selective ligands, which might possess unique therapeutic value for opioid addiction treatment.



## INTRODUCTION

Opium, the dried latex obtained from the immature seedpod of a poppy flower (*Papaver somniferum*), has been used for medical and euphoric purposes since ancient time. The major active ingredient was later identified to be morphine (Figure 1).<sup>1</sup> Opioids is a generic term referring to alkaloids isolated from opium poppy, their synthetic analogues, and endogenous substances synthesized in the human body.<sup>2</sup> Opioids exert their function through interacting with one or more of the three major opioid receptors, designated as the mu opioid receptor (MOR), the kappa opioid receptor (KOR), and the delta opioid receptor (DOR).<sup>3,4</sup> Among them, the MOR plays a major role in mediating the antinociception and other unwanted adverse effects of opioids, such as abuse/addiction liability, respiratory depression, sedation, and constipation.<sup>5</sup> Among the side effects, the abuse/addiction liability is the major concern for prescription of opioid analgesics.

According to the 2012 World Drug Report, the global annual prevalence of illicit opioids use ranged from 0.6 to 0.8% of the adult population in 2010. North America (3.8–4.2%), Oceania (2.3–3.4%), and Eastern and South-Eastern Europe (1.2–1.3%) have a higher prevalence of illicit opioid use than the global average. The nonmedical use of prescription opioids plays a dominant and problematic role in North America. For the United States alone, the overdose deaths involving

prescription opioids in 2010 was four times that in 1999.<sup>2</sup> Therefore, efficacious medications are still highly desired to treat acute (overdose) and chronic (abuse/addiction) side effects of opioids.

The current FDA approved pharmacologic treatment for long-term opioid dependence/addiction based on the MOR mechanisms includes methadone (a full agonist), buprenorphine (a partial agonist), and naltrexone (an antagonist) (Figure 1).<sup>6–8</sup> Although methadone has shown great efficacy for opioid-addiction maintenance, it could cause lethal respiratory depression when taken in overdose because of its MOR full-agonist property.<sup>6</sup> Furthermore, sudden cessation of methadone would precipitate a longer period of withdrawal symptoms than that following morphine termination, which has led to methadone becoming an abused drug itself.<sup>9</sup> Similarly, buprenorphine also suffered the same drawbacks of methadone, albeit to a lesser extent because of its partial agonism on the MOR,<sup>10</sup> whereas it was associated with fewer drug–drug interactions compared to methadone.<sup>6</sup> In contrast, as a MOR antagonist, naltrexone did not induce respiratory suppression and showed no abuse liability. However, it has precipitated considerable withdrawal syndrome, which has compromised its

Received: August 7, 2013

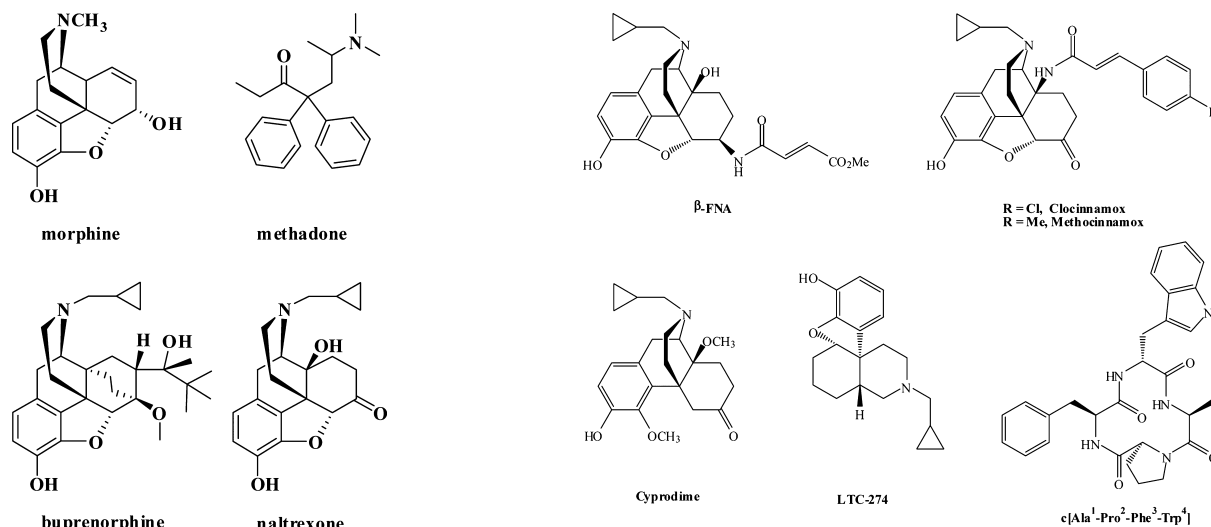
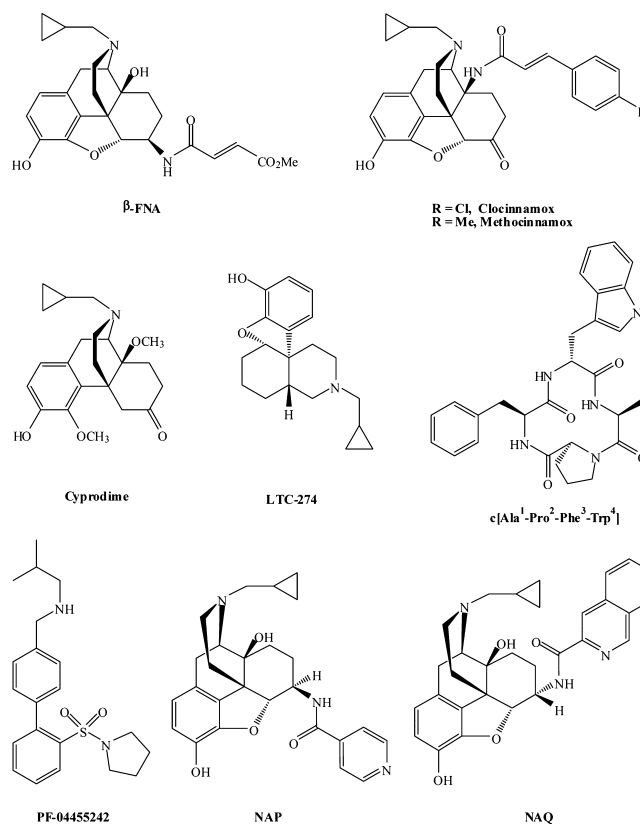


**Figure 1.** Morphine and the current available drugs for opioid dependence/addiction treatment based on the MOR mechanisms.

therapeutic efficiency.<sup>11–14</sup> The extended-release formulation of naltrexone significantly improved the adherence rate and treatment outcome.<sup>15,16</sup> Nevertheless, its application is restricted from people who have end-stage liver disease or who need a long period of chronic pain management.<sup>6</sup> Collectively, these three drugs have associated shortcomings, although they do serve as proof-of-concept that targeting the MOR could provide effective treatment for opioid dependence and addiction.

In this respect, a number of chemical entities have been developed as MOR ligands. Some of the representatives are depicted in Figure 2. Among them,  $\beta$ -funaltrexamine ( $\beta$ -FNA), clocinnamox, and methocinnamox are potential MOR irreversible antagonists.  $\beta$ -FNA binds with equal potency to the MOR and KOR, whereas clocinnamox and methocinnamox bind to all three opioid receptors in mouse brain homogenates with similar affinity.<sup>17</sup>  $\beta$ -FNA also possessed reversible KOR agonist activity.<sup>18–20</sup> Cyprodime is another intensively studied MOR antagonist, which has moderate selectivity and potency at the MOR ( $K_i$  value ratios are  $\delta/\mu \approx 39$  and  $\kappa/\mu \approx 10$ ;  $K_i$  at the MOR is  $10.6 \pm 0.7$  nM).<sup>21,22</sup> Sally et al. recently disclosed (–)-3-cyclopropylmethyl-2,3,4,4 $\alpha$ ,5,6,7,7 $\alpha$ -octahydro-1H-benzofuro[3,2-e]isoquinolin-9-ol (LTC-274)<sup>23</sup> (Figure 2) as a novel MOR antagonist, which showed the least inverse agonist activity at the MOR among 21 ligands tested. Meanwhile, this compound bound to the KOR as strongly as to the MOR, and it acted as a KOR partial agonist ( $EC_{50} = 2.7$  nM,  $E_{max} = 23\%$ ).<sup>23</sup> 2-Methyl-N-([2'-(pyrrolidin-1-ylsulfonyl)-biphenyl-4-yl]methyl)propan-1-amine (PF-04455242)<sup>24</sup> and c[Ala<sup>1</sup>-Pro<sup>2</sup>-Phe<sup>3</sup>-Trp<sup>4</sup>]<sup>25</sup> (a cyclic peptidyl derivative) have also been reported to function as MOR/KOR dual antagonists (Figure 2). However, both of them were more potent and selective at the KOR.<sup>24,25</sup> Therefore, MOR-selective ligands with high potency are still highly desirable.

From another standpoint, accumulating evidence shows that the release of dynorphins and the activation of the KOR mediates dysphoria and anhedonia associated with drug withdrawal, stress-induced aversion states, and stress-induced relapselike behavior.<sup>26</sup> For example, the KOR-selective agonist 2-(3,4-dichlorophenyl)-N-methyl-N-[(1R,2R)-2-pyrrolidin-1-ylcyclohexyl]acetamide **1** (U50,488) mimicked stress exposure

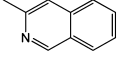
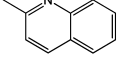
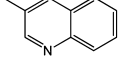
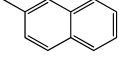


**Figure 2.** Representatives of the small molecules possessing MOR-antagonist characteristics.

and significantly potentiated cocaine-conditioned place preference.<sup>27</sup> Furthermore, **1** effectively reinstated cocaine-seeking behavior in mice previously conditioned to cocaine.<sup>28</sup> Such effects of **1** were abolished by the KOR-selective antagonist nor-binaltorphimine (norBNI) in both studies.<sup>27,28</sup> Meanwhile, it has also been reported that blockade of the dynorphin/KOR system decreased dependence-induced ethanol self-administration in male Wistar rats.<sup>29</sup> In contrast, the effects of the dynorphin/KOR system on opioid dependence and addiction seemed to be dose-, ligand-, and species-specific. For instance, low doses of **1** first increased (0.1 mg/kg) and then decreased (0.5 mg/kg) heroin self-administration in mice.<sup>30</sup> KOR-selective agonist (2E)-N-[(5 $\alpha$ ,6 $\beta$ )-17-(cyclopropylmethyl)-3,14-dihydroxy-4,5-epoxymorphinan-6-yl]-3-(3-furyl)-N-methylacrylamide (TRK-820) but not N-methyl-2-phenyl-N-[(5R,7S,8S)-7-(pyrrolidin-1-yl)-1-oxaspiro[4.5]dec-8-yl]-acetamide (U69,593) decreased morphine-induced conditional place preference.<sup>31,32</sup> NorBNI potentiated naloxone-precipitated morphine-withdrawal symptoms in rats,<sup>33</sup> whereas KOR gene disruption in mice showed reduced naloxone-precipitated morphine-withdrawal syndrome.<sup>34</sup> Collectively, these data implicated that the dynorphin/KOR system may act as an important modulator in the neurobiology of drug dependence and addiction, and it could serve as a cotarget along with the MOR for drug dependence and addiction treatment.<sup>35–37</sup>

The continuing interest in developing novel, nonpeptidic, and reversible opioid receptor ligands in our lab led to the identification of two potent and highly selective MOR ligands, NAP and NAQ, the C6-heteroaromatic-substituted naltrexone derivatives based on a MOR homology model and the “message-address” concept (Figure 2).<sup>38</sup> Both compounds

**Table 1. Opioid Receptor Binding Affinity, Selectivity, and the MOR [<sup>35</sup>S]-GTPγS Functional Assay Results of the First Generation of 14-Substituted Naltrexone Derivatives<sup>a</sup>**

Compd	R	<i>K<sub>i</sub></i> (nM)			Selectivity			% <i>E<sub>max</sub></i> of DAMGO
		<i>μ</i>	<i>κ</i>	<i>δ</i>	<i>κ/μ</i>	<i>δ/μ</i>	<i>δ/κ</i>	
NTX	NA	0.26 ± 0.02	5.15 ± 0.26	117.0 ± 8.9	20	450	23	ND
2 (ONP)		0.14 ± 0.03	25.5 ± 6.5	117.4 ± 18.0	182	838	4.6	ND
3		1.59 ± 0.61	47.8 ± 8.5	170.3 ± 12.6	30	107	3.6	ND
4		5.58 ± 1.34	49.2 ± 20.4	405.3 ± 234.7	8.8	73	8.2	ND
5 (control)		123.2 ± 38.2	586.4 ± 32.4	>10,000.00	4.7	>81	>17	ND
6		68.4 ± 6.0	>10,000	>10,000	>146	>146	NA	ND
7		1.44 ± 0.32	67.2 ± 36.7	22.8 ± 19.5	47	16	0.34	ND
8		2.69 ± 0.72	148.2 ± 55.5	818.4 ± 507.2	55	304	5.5	22.0 ± 10.3
9 (control)		225.3 ± 46.6	46.6 ± 13.5	907.2 ± 193.0	0.21	4.0	19	ND

<sup>a</sup>The values are the means ± SEM of three independent experiments. [<sup>3</sup>H]NLX, [<sup>3</sup>H]NTI, and [<sup>3</sup>H]norBNI were used to label MOR, DOR and KOR, respectively. The percentage stimulation to DAMGO is the *E<sub>max</sub>* of the compound compared to that of 3 μM DAMGO (normalized to 100%). NA, not applicable. ND, not detectable.

acted as MOR partial agonists with low efficacy in the [<sup>35</sup>S]-GTPγS binding assay but antagonized the effects of the MOR full agonists both in vitro and in vivo.<sup>38,39</sup> Docking experiments of naltrexone to the same MOR homology model led to the identification of an alternative “address” domain that is located around extracellular loop III and the upper-level region of transmembrane VI/VII,<sup>40</sup> which might have the potential to interact with some putative substitutions at the 14-position of naltrexone to increase the MOR-binding affinity and selectivity. To test this hypothesis, three generations of 14-heteroaromatic-substituted naltrexone derivatives were designed and synthesized consecutively. All of the newly synthesized compounds were tested in the opioid receptor radioligand competition binding assay and in the [<sup>35</sup>S]-GTPγS binding assay for their affinity, selectivity, and function. Selected compounds were further evaluated for the acute antinociceptive agonistic/antagonistic effects in the tail-flick assay as well as for the opioid-withdrawal symptoms in morphine-dependent mice. Two representative ligands were also docked into the crystal structures of three opioid receptors to validate further our original hypothesis.

## RESULTS AND DISCUSSION

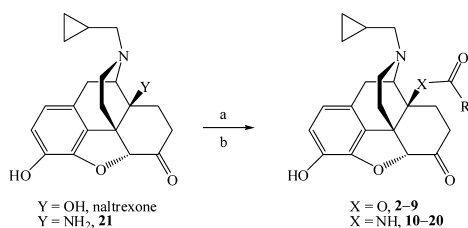
**Molecular Design.** A previous molecular-modeling study revealed that the 14-hydroxyl group of naltrexone might putatively point to some nonconserved yet potential hydrogen-

bond donor/acceptor residues (i.e., Tyr210 and Trp318) in one of the MOR-naltrexone binding modes,<sup>40</sup> which might be able to act as a unique MOR address domain. We thus hypothesized that a functionalized moiety that could interact with these residues (through hydrogen bonding and/or aromatic stacking) might provide enhanced MOR affinity and thus increase the MOR selectivity over the KOR and the DOR. Six heteroaromatic ring side chains containing one nitrogen atom (a hydrogen-bond donor under physiological conditions) and two aromatic rings (as the control compounds) were chosen to test this hypothesis. These functionalized moieties were introduced to the 14-hydroxyl group of naltrexone via an ester bond (compounds 2–9) based on a straightforward chemical synthetic method. Compound 2 was then identified as the most selective MOR molecule among the first-generation ligands. However, there have been reports that sterically hindered tertiary esters (such as compounds 2–9) could possibly be hydrolyzed by certain esterases and lipases.<sup>41,42</sup> To avoid such potential shortcomings and also to facilitate future in vivo studies, the isosteres of compounds 2–9, amide analogues 10–17, were then synthesized as the second-generation compounds to test whether the high MOR selectivity induced by these heteroaromatic ring would be retained. Interestingly, the amide derivatives became selective to both the MOR and the KOR. Among them, ligand 10 appeared to have the highest selectivity for these two receptors over the DOR. To investigate

whether the selectivity-profile change for ligand **10** was due to different projection of the 2'-pyridyl ring as a result of the restricted rotation of the amide bond compared to the ester linkage, different lengths of spacers were introduced between the epoxymorphinan skeleton and the 2'-pyridyl ring in compound **10** to yield the third-generation compounds **18–20**. Surprisingly, these ligands with an extended spacer were still MOR/KOR dual selective. This suggested that the amide bond itself might be involved in the receptor–ligand interactions, which was later supported by our molecular-modeling study based on the crystal structures of three opioid receptors.

**Chemistry. Synthesis of 14-Substituted Naltrexone Derivatives.** The 14-O-substituted naltrexone derivatives (**2–9**, Table 1) were readily obtained by reacting naltrexone with the corresponding acyl chloride in TEA/DMF at 100 °C with subsequent saponification under either acidic (compounds **2–4** and **6–8**) or basic (compounds **5** and **9**) conditions (Scheme 1).<sup>40</sup>

**Scheme 1. Synthetic Route of the Three Generations of 14-Substituted Naltrexone Derivatives 2–20<sup>a</sup>**



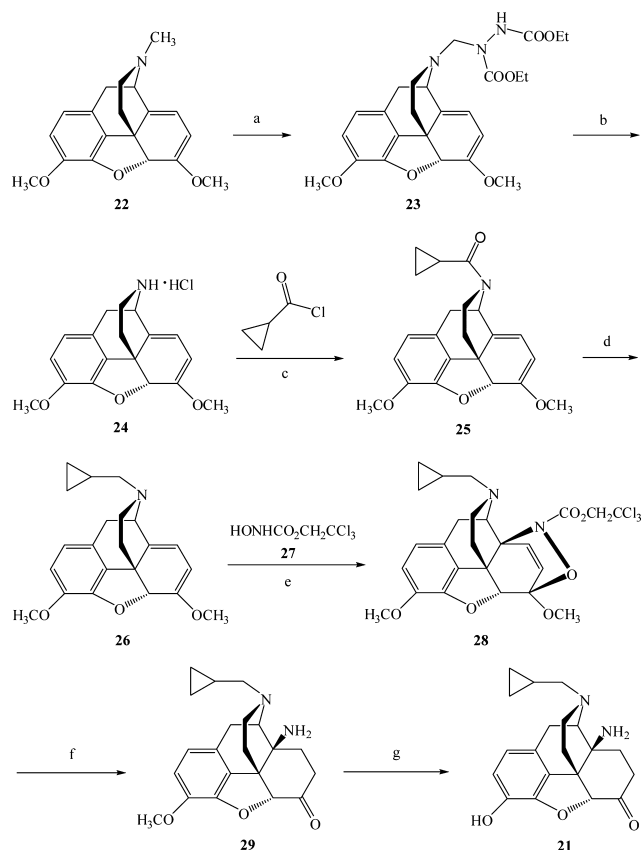
<sup>a</sup>(a) RCOCl or RCOOH; (b) K<sub>2</sub>CO<sub>3</sub> or H<sub>2</sub>SO<sub>4</sub>.

An established synthetic route shown in Scheme 2 was adopted to prepare 14-aminonaltrexone **21**.<sup>43</sup> Compounds **10–20** were then obtained by coupling intermediate **21** with an acid/acyl chloride, commercially available or prepared in house (see the Supporting Information), followed by saponification with K<sub>2</sub>CO<sub>3</sub> as described previously (Scheme 1).<sup>38,43,44</sup>

**Biology. In Vitro and in Vivo Pharmacological Studies.** The synthesized three generations of naltrexone derivatives were first evaluated in the radioligand competition binding assay and in the [<sup>35</sup>S]-GTPγS functional assay on opioid receptor-transfected CHO cell membranes for their binding affinity, selectivity, and MOR agonism/antagonism (in vitro). Then, selected compounds were further advanced to behavioral tail-flick and opioid-withdrawal assays for their functional activity (in vivo). Naltrexone (NTX) was tested along for comparison in all of the assays.

**In Vitro Radioligand Binding Assay and [<sup>35</sup>S]-GTPγS Functional Assay.** The competitive radioligand binding assay was performed on monoclonal opioid receptor-expressed CHO cell membranes as described previously.<sup>38,39,44</sup> [<sup>3</sup>H]naloxone (NLX), [<sup>3</sup>H]naltrindole (NTI), and [<sup>3</sup>H]norBNI (for compounds **2–9**) or [<sup>3</sup>H]diprenorphine (DPN, for compounds **10–20**) were used to label the MOR, DOR, and KOR, respectively. The MOR [<sup>35</sup>S]-GTPγS binding assay was conducted to determine whether each of the new ligands would act as a full agonist, a partial agonist, or an antagonist at the MOR, as illustrated before.<sup>38,39,44</sup> The results were interpreted as the relative efficacy of each compound to a MOR full agonist [<sup>D</sup>-Ala<sup>2</sup>-MePhe<sup>4</sup>-Gly(ol)<sup>5</sup>]enkephalin (DAMGO) for MOR activation.

**Scheme 2. Synthetic Route of 14-Aminonaltrexone 21<sup>a</sup>**



<sup>a</sup>(a) DEAD, benzene, reflux; (b) pyridine·HCl, EtOH/H<sub>2</sub>O, reflux to rt, 83%, two steps; (c) TEA, DCM, 0 °C to rt, quantitative; (d) LiAlH<sub>4</sub>, THF, reflux, 77%; (e) NaIO<sub>4</sub>, NaOAc, EtOAc, 73%; (f) Pd/C, H<sub>2</sub>/60 psi, AcOH, NaOAc, MeOH, 40%; (g) BBr<sub>3</sub>, DCM, 44%.

As seen in Table 1, all of the first generation of naltrexone derivatives retained subnanomolar to one-digit nanomolar binding affinity at the MOR except for compounds **5**, **6**, and **9**. The relatively low binding affinity of control compounds **5** and **9** compared to the rest of the ester congeners indicated that the nitrogen atom in the functionalized moiety of these derivatives did play an important role in the MOR–ligand interactions. In detail, nitrogen atom substitutions with 2',3'-pyridyl (compounds **2** and **3**, respectively) and 2',3'-quinolyl (compounds **7** and **8**, respectively) were favorable for MOR binding (11–40-fold higher compared to other isomers). Meanwhile, the first generation of naltrexone derivatives generally all displayed considerably decreased binding affinities at the KOR and DOR compared to naltrexone (except for compounds **2** and **7** at the DOR), and compounds **2**, **3**, **6**, and **8** showed a greater than 30-fold selectivity to the MOR over the KOR and the DOR. In this sense, the nitrogen atom position seemed to be critical as well. Compound **2** (ONP) appeared to be the most selective and potent MOR ligand in this first generation of naltrexone derivatives. As for the MOR [<sup>35</sup>S]-GTPγS binding assay, all of the first-generation compounds, except for ligand **8**, did not show any detectable MOR agonism under the tested conditions.

In contrast, the second generation of naltrexone derivatives (**10–17**) also bound to the MOR at subnanomolar to one-digit nanomolar affinity (Table 2). However, the presence/absence and the position of the nitrogen atom in the functionalized

Table 2. Opioid Receptor Binding Affinity, Selectivity, and MOR [<sup>35</sup>S]-GTPγS Functional Assay Results of the Second and Third Generations of 14-Substituted Naltrexone Derivatives<sup>a</sup>

Compd	R	K <sub>i</sub> (nM)			Selectivity			% E <sub>max</sub> of DAMGO
		μ	κ	δ	μ/κ	δ/κ	δ/μ	
NTX	NA	0.34 ± 0.03	0.90 ± 0.11	95.5 ± 6.1	0.4	106	281	7.2 ± 0.6
10 (NNP)		1.51 ± 0.34	0.36 ± 0.01	94.5 ± 6.5	4.2	263	63	0.9 ± 0.4 <sup>b</sup>
11		0.75 ± 0.28	0.16 ± 0.01	39.9 ± 0.5	4.7	249	53	5.1 ± 0.6 <sup>b</sup>
12		0.82 ± 0.33	0.33 ± 0.01	10.9 ± 1.3	2.5	33	13	7.7 ± 0.7
13 (control) <sup>c</sup>		4.34 ± 0.70	0.12 ± 0.001	57.3 ± 4.3	36	477	13	5.8 ± 1.4
14		3.50 ± 1.87	0.27 ± 0.02	25.1 ± 1.8	13	93	7.2	2.8 ± 1.6 <sup>b</sup>
15		9.09 ± 4.94	0.26 ± 0.01	15.1 ± 0.6	35	58	1.7	34.4 ± 5.4
16		1.13 ± 0.25	0.13 ± 0.02	1.48 ± 0.05	8.7	11	1.3	15.8 ± 5.6
17 (control) <sup>c</sup>		6.22 ± 4.01	0.33 ± 0.02	10.5 ± 1.4	19	32	1.7	16.5 ± 2.0
18		0.29 ± 0.04	0.19 ± 0.03	3.92 ± 0.12	1.5	21	14	78.0 ± 2.7
19		0.32 ± 0.04	0.17 ± 0.02	9.1 ± 0.5	1.9	54	29	12.7 ± 0.2
20		0.30 ± 0.01	0.14 ± 0.01	0.37 ± 0.04	2.1	2.6	1.2	11.8 ± 0.4

<sup>a</sup>The values are the means ± SEM of three independent experiments. [<sup>3</sup>H]NLX, [<sup>3</sup>H]NTI, and [<sup>3</sup>H]DPN were used to label MOR, DOR, and KOR, respectively. The percentage stimulation to DAMGO is the E<sub>max</sub> of the compound compared to that of 3 μM DAMGO (normalized to 100%). NA, not applicable. <sup>b</sup>Percentage stimulation produced at the maximum concentration of 10 μM. <sup>c</sup>These controls were also reported previously in ref 57.

moiety did not seem to have a significant impact on their MOR binding affinity. In the meantime, increased binding affinities at the KOR and DOR were observed for these second-generation compounds 10–17 in comparison to both naltrexone and the first-generation ligands, which significantly changed their opioid-receptor-selectivity profile. Some of the ligands were both MOR and KOR selective over the DOR (compounds 10–12), whereas others were even more KOR selective over the MOR and the DOR (compounds 13–15 and 17). Nevertheless, the majority of the second generation of naltrexone derivatives produced less than 20% MOR stimulation relative to DAMGO. Compounds 10 (NNP), 11, and 14 showed relatively lower MOR efficacy among this series of compounds. Compared to the undetectable MOR agonism of the first-generation ligands, the isostere replacement of an ester linkage with an amide bond not only decreased MOR selectivity over the KOR but also slightly enhanced ligand MOR efficacy.

Compounds 18–20 were then prepared to test whether the changed opioid receptor selectivity was due to the restricted rotation of the amide bond compared to the ester linkage. As shown in Table 2, ligands 18 and 19 were still MOR/KOR dual selective, whereas ligand 20 bound to all three opioid receptors with nearly equal potency. It thus seemed that the conventionally restricted rotation of the amide bond might not be the reason for the ligand opioid receptor-selectivity change from MOR (ligand 2) to MOR/KOR (ligand 10). Meanwhile, the relative lower K<sub>i</sub> values of ligands 18–20 with an extended spacer compared to that of ligand 10 suggests that a less restricted functionalized moiety could facilitate ligand binding to the MOR. Ligand 18 behaved as a MOR partial agonist with relatively high efficacy, whereas ligands 19 and 20 acted as low-efficacy MOR partial agonists.

Collectively, the radioligand competition binding assay identified three potent MOR selective ligands (2, 3, and 8)

and three potent MOR/KOR dual-selective ligands (**10**, **11**, and **19**). These six novel ligands all displayed marginal MOR agonism in the [<sup>35</sup>S]-GTPγS binding assay. We noticed that a similar opioid-receptor-selectivity profile change upon isosterism has also been reported for methocinamox (amide linkage) and its ester analogue. Methocinamox has no selectivity among the three opioid receptors, whereas its ester analogue is moderately selective to the MOR over the KOR and the DOR. (The  $K_i$  value ratios for methocinamox are  $\delta/\mu \approx 1$  and  $\kappa/\mu \approx 3$  and for its ester isostere are  $\delta/\mu \approx 31$  and  $\kappa/\mu \approx 15$ .)<sup>45</sup> Such findings somewhat coincided with our observation of the selectivity-profile change reported herein.

Because compounds **10** and **11** showed relatively higher MOR/KOR dual selectivity over the DOR among all of the new ligands, the [<sup>35</sup>S]-GTPγS binding assays of these two compounds on the monoclonal KOR and DOR-expressed CHO cell membranes were further conducted. Compound **14** was also included in these assays because of its minimal efficacy at the MOR (Table 3). Naltrexone and compounds **10** and **14**

**Table 3.** KOR/DOR [<sup>35</sup>S]-GTPγS Binding Results for Compounds **10**, **11**, and **14**<sup>a</sup>

compound	KOR [ <sup>35</sup> S]-GTPγS binding		DOR [ <sup>35</sup> S]-GTPγS binding	
	EC <sub>50</sub> (nM)	% E <sub>max</sub> of <b>1</b>	EC <sub>50</sub> (nM)	% E <sub>max</sub> of <b>30</b>
NTX	0.81 ± 0.08	20.8 ± 0.9	4.4 ± 1.6	5.6 ± 0.6
<b>10</b> (NNP)	1.74 ± 0.50	24.9 ± 2.0	19.7 ± 7.4	8.6 ± 0.8
<b>11</b>	0.56 ± 0.06	35.3 ± 6.8	3.2 ± 2.0	10.3 ± 0.6
<b>14</b>	2.75 ± 0.71	16.8 ± 0.6	14.2 ± 1.9	23.8 ± 0.7

<sup>a</sup>The values are the means ± SEM of three independent experiments. The percentage stimulation to **1** or **30** is the E<sub>max</sub> of the compound compared to that of **1** or **30** (normalized to 100%).

appeared to carry similar efficacy at the KOR, whereas compound **11** appeared to show the highest efficacy. However, naltrexone and compounds **10** and **11** exhibited marginal efficacy at the DOR, whereas compound **14** showed the highest efficacy, although its potency was relatively low.

**Tail-Flick Assay.** Because of their minimum MOR activation, as shown in the [<sup>35</sup>S]-GTPγS functional assay, compounds **10**, **11**, and **14** were chosen for further evaluation of their acute agonistic and antagonistic effects in the tail-flick assay in mice. None of the compounds produced any significant agonist effect up to a 30 mg/kg dose, although they were found to potentially antagonize the analgesic effect of morphine (Table 4). Compound **10** seemed to be the most potent among these three new ligands. In general, the in vivo assay results were consistent with the in vitro MOR [<sup>35</sup>S]-GTPγS functional data for these compounds.

**Table 4.** AD<sub>50</sub> Values of Compounds **10**, **11**, and **14** for Antagonizing the Morphine (10 mg/kg) Antinociception Effect in a Warm-Water Tail-Flick Assay<sup>a</sup>

compound	AD <sub>50</sub> values (mg/kg (95% CL))
naloxone	0.05 (0.03–0.09)
naltrexone	0.006 (0.003–0.014)
<b>10</b> (NNP)	0.25 (0.18–0.36)
<b>11</b>	0.55 (0.35–0.87)
<b>14</b>	0.87 (0.52–1.47)

<sup>a</sup>All drugs and test compounds were administered to a group of six mice subcutaneously (s.c.).

**Opioid-Withdrawal Assays.** Because the ultimate goal of the study is to identify selective opioid receptor ligands for opioid dependence and addiction treatment, it is necessary to evaluate whether these new ligands would precipitate severe withdrawal symptoms in morphine-dependent mice (Figure 3).

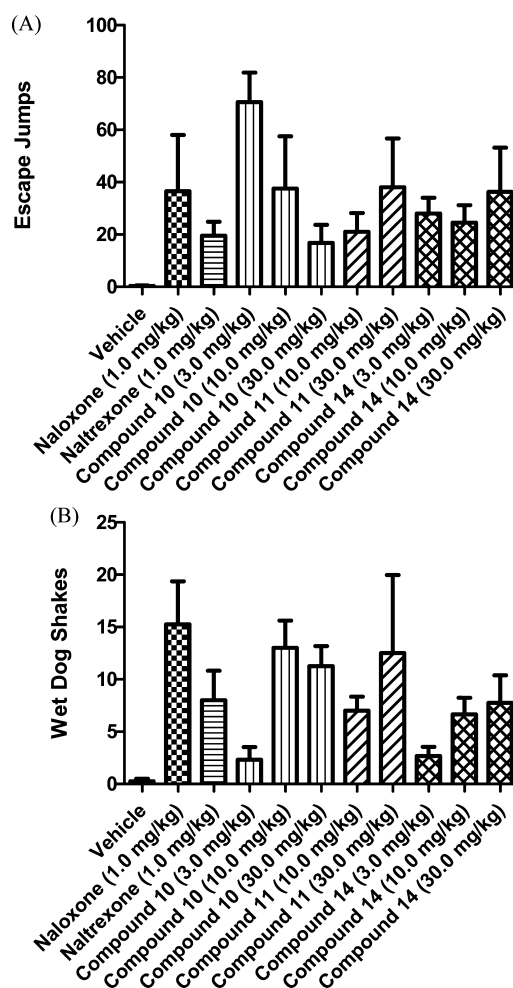


**Figure 3.** 14-N-Heteroaromatic-substituted naltrexone derivatives **10**, **11**, and **14** in withdrawal assays in chronic morphine-exposed mice: (A) escape jumps and (B) wet dog shakes.

Similar to previous reports,<sup>39,46</sup> the well-known opioid antagonist naltrexone precipitated significant withdrawal syndrome, which was manifested by the number of escape jumps (over 20; Figure 3A) and wet dog shakes (7; Figure 3B) in morphine-pelleted mice, whereas naloxone showed even more significant syndrome (Figure 3). Interestingly, in the first assay, compound **10** displayed a clear decrease in escape jumps as its dose increased (although this was not significant), with similar jumping numbers at 30 mg/kg to that of 1 mg/kg of naltrexone (Figure 3A). In contrast, there seemed to be an increasing dose–response effect for compound **11** and no significant dose–response effect for compound **14**, respectively. Compounds **11** and **14** at 30 mg/kg yielded a similar number of jumps as that produced by 1 mg/kg naloxone.

There was a minimal number of wet dog shakes for compound **10** at 3 mg/kg, but a dramatic increase was observed as the dose went up to 10 mg/kg, which remained at the same level at 30 mg/kg. Nevertheless, the effects at high doses of compound **10** were still lower than that of 1 mg/kg naloxone

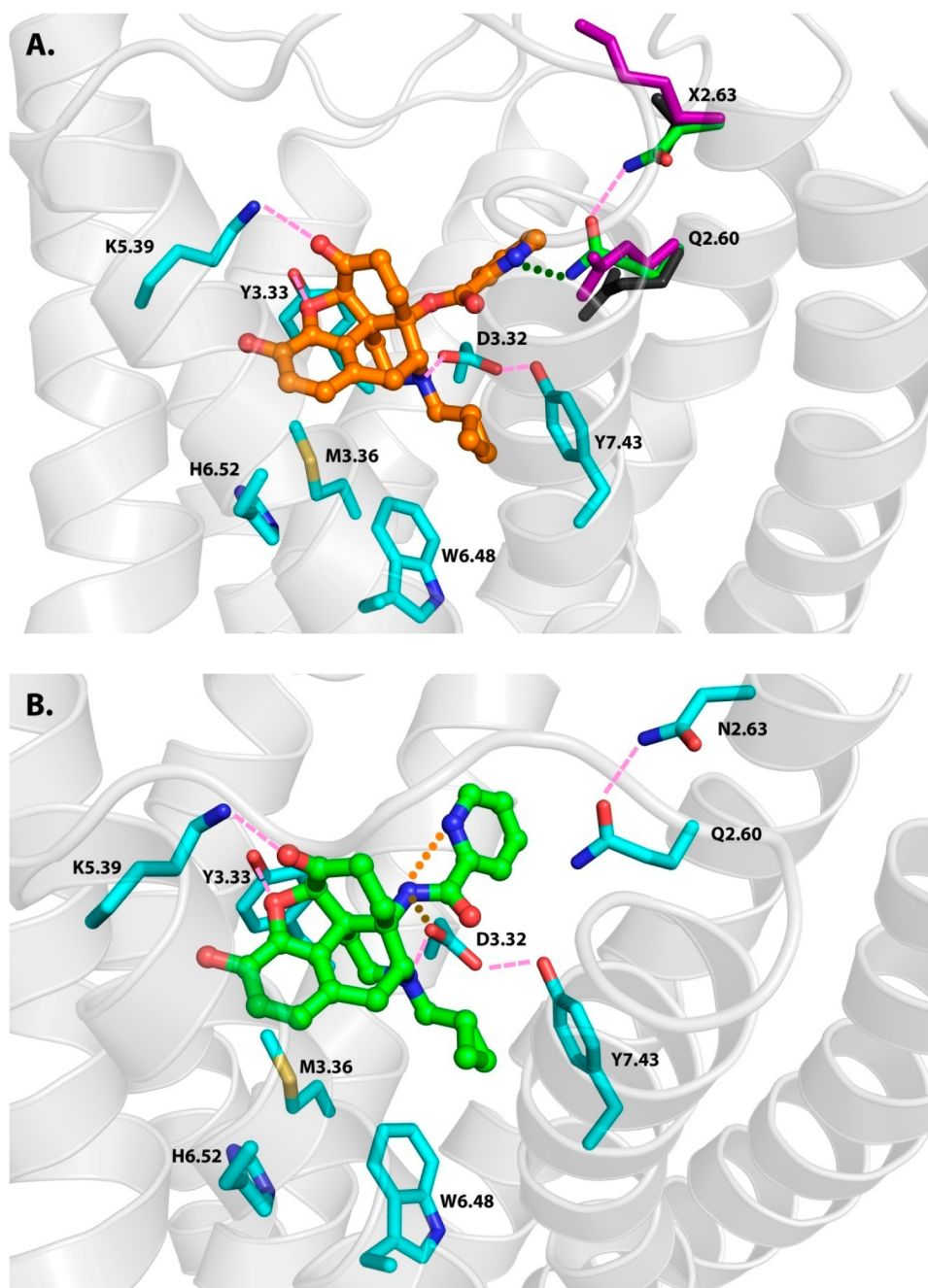


**Figure 4.** (A) Superimposed binding mode of ligand **2** (orange balls and stick) in three opioid receptors: conserved residues (cyan), MOR residues (green), KOR residues (black), and DOR residues (purple). Pink dashes and green dots represent possible hydrogen-bonding interactions. Asn<sup>2.63</sup> (MOR), but not Val<sup>2.63</sup> (KOR) or Lys<sup>2.63</sup> (DOR), facilitated the hydrogen-bonding interaction (green dots) between Gln<sup>2.60</sup> and the pyridyl nitrogen atom. The formed hydrogen-bonding network yields the high MOR selectivity of ligand **2** over the KOR and DOR. (B) Highest-scored binding mode of ligand **10** (green balls and stick) in the MOR (cyan). Conserved hydrogen-bonding interactions, as seen for ligand **2**, are shown in pink dashes. A potential internal hydrogen bond (orange dots) between the amide NH and the pyridyl nitrogen in ligand **10** disrupts the hydrogen-bonding network, as observed for ligand **2**. Furthermore, a hydrogen-bonding interaction (brown dots) also formed between the amide NH and the conserved residue Asp<sup>3.32</sup> in all three opioid receptors and thus enhanced the binding affinities of ligand **10** in all three opioid receptors. Together, a reduced MOR selectivity for ligand **10** was observed as compared to that of ligand **2**.

(Figure 3B). Both compounds **11** and **14** appeared to show an increasing dose–response effect with the wet dog shakes, whereas at their highest doses tested (30 mg/kg) they resembled the effect of 1 mg/kg naloxone and naltrexone. Because all three compounds only showed marginal efficacy at the MOR, their partial agonism at the KOR and DOR could be one of the factors for their distinct profiles in the withdrawal assays. Nevertheless, the withdrawal symptoms of these MOR/

KOR dual-selective ligands seemed to be less significant than naloxone, which sheds some light on their potential application in drug-abuse/addiction treatment.

**Molecular-Modeling Study.** As discussed earlier, the selectivity profile of the first and second generations of naltrexone derivatives switched from MOR selective (ester analogues) to MOR/KOR dual selective (amide analogues). To understand this phenomena in the context of ligand–receptor

interaction, automated docking of ligands **2** and **10** (the two compounds that showed the highest selectivity in each generation) to the crystal structures of three opioid receptors<sup>47–49</sup> was performed by employing GOLD5.1. In the majority of the obtained docking modes, the known morphinan-type pose was scored the highest for both ligands, and the docking poses of ester bond-linked ligand **2** were similar to those of amide bond-linked ligand **10**.

To identify the possible explanations for the high MOR selectivity of ligand **2** over the KOR and DOR, amino acid residues around the binding pocket for each opioid receptor along with docked ligand **2** were allowed to attain a lower-energy conformation by a 10 ps NVT dynamic simulation (moles, N, volume, V, and temperature, T, are conserved) at 300 K under TRIPOS force field (TFF). After averaging the last 1 ps of the simulation, the obtained energy-minimized structures were then studied. Interestingly, conformational changes observed for Gln<sup>2.60</sup> of the MOR allowed for a possible hydrogen-bonding interaction with the pyridyl nitrogen of ligand **2** (Figure 4A, green dots). However, this conserved Gln residue was directed differently in both the KOR and DOR, diminishing the possibility of hydrogen-bonding interactions between the Gln residue and the pyridyl nitrogen of ligand **2** in these two receptors (Figure 4A). Looking further within the same docking pocket, it was noticed that the residues at position 2.63 (directly above Gln<sup>2.60</sup>) for the three opioid receptors projected and functioned differently. Asn<sup>2.63</sup> in the MOR presented a helical turn above Gln<sup>2.60</sup> and helped to direct Gln<sup>2.60</sup> toward ligand **2** through a hydrogen bond (Figure 4A, pink dashes). However, for the KOR and DOR, the 2.63 position was occupied by Val118 and Lys108, respectively, which were not able to interact with the Gln<sup>2.60</sup> residue through hydrogen bonds (Figure 4A). On the basis of the receptor competition binding assay results and the current modeling studies, we hypothesized that a hydrogen-bonding network among the pyridyl nitrogen of ligand **2**, the conserved Gln residue at 2.60 position, and the nonconserved residue at 2.63 position of the three opioid receptors is responsible for the receptor selectivity of this ligand. The presence of such a hydrogen-bonding network enables ligand **2** to be more MOR selective over the KOR and DOR.

In contrast, the MOR selectivity over the KOR was lost for ligand **10** even though it has the same functionalized moiety as ligand **2**. To understand the possible conformational changes in residues around the binding pocket that might cause the decreased MOR selectivity for ligand **10**, the ester O atom of ligand **2** was replaced with amide NH atoms to put ligand **10** in the same docking pose as ligand **2**. This was then followed by the same dynamic simulation experiment as described earlier. Figure 4B presents the highest-scored binding mode of ligand **10** in the MOR. The model suggested that for ligand **10**, because of a possible internal hydrogen bond between the amide NH and the pyridyl nitrogen (Figure 4B, orange dots), the pyridyl nitrogen preferred to stay close to the amide NH (potential energy under TRIPOS force field calculated for ligand **10** pose with the internal hydrogen bond was 12.5 kcal/mol lower than that without the internal hydrogen bond). Thus, the pyridyl nitrogen was no longer available to form a hydrogen bond with the Gln<sup>2.60</sup>, which seemed to be a key component of the hydrogen-bonding network that decided the opioid receptor selectivity of ligand **2** according to our observation. Furthermore, this internal hydrogen bond in ligand **10** also facilitated the amide NH to form a hydrogen-

bonding interaction (Figure 4B, brown dots) with the conserved residue Asp<sup>3.32</sup> in all three opioid receptors, which would enhance the binding affinities of ligand **10** to all three opioid receptors. Therefore, disruption of the hydrogen-bonding network and formation of a hydrogen bond with a conserved residue in all three opioid receptors together might account for the reduced MOR selectivity for ligand **10** compared to its ester isostere ligand **2**.

Taken together, the current molecular-modeling study based on the crystal structures of three opioid receptors identified an alternative MOR address domain composed of Gln<sup>2.60</sup> and Asn<sup>2.63</sup> in transmembrane helix II. Interestingly, such finding is significantly different from our previous studies that applied opioid receptor homology models based on the crystal structure of bovine rhodopsin. Similar discrepant results have also been observed by other research groups.<sup>50</sup> We also noticed that the introduction of a substitution at the 14-position of morphinan skeleton could be crucial in altering the pharmacological profile,<sup>51</sup> whereas the orientation (in the manner of rotation freedom) of such a substitution at this position may lead to high-potency MOR-agonism activity during the development of some pseudoirreversible opioid receptor antagonists.<sup>52–54</sup> In combination with our observations, a more vivid picture of the impact of 14-substitution on the pharmacology of the morphinan skeleton derivatives is now available.

## CONCLUSIONS

On the basis of a previous MOR homology model, three generations of 14-heteroaromatic-substituted naltrexone derivatives (esters **2–9** and amides **10–20**) were designed, synthesized, and biologically evaluated. The majority of these new ligands bound to the MOR with subnanomolar to nanomolar affinity. The selectivity profile of the compounds switched from MOR selective to MOR/KOR dual selective upon application of the concept of isosterism, with a marginal increase of the functional activity in the MOR [<sup>35</sup>S]-GTPγS binding assay. Further molecular-modeling studies based on the crystal structures of three opioid receptors revealed that a hydrogen-bonding network among the functionalized moiety (a nitrogen atom on an aromatic-ring system), the Gln residue at the 2.60 position, and the nonconserved residue at the 2.63 position might decide the opioid receptor selectivity of these ligands. The presence of such a network led to high MOR selectivity over the KOR and DOR for ligand **2** (ONP). Among the amide series of naltrexone derivatives, compounds **10**, **11**, and **14** showed minimal MOR efficacy in the [<sup>35</sup>S]-GTPγS binding assay. These three compounds also had no agonist-like property and acted as potent MOR antagonists in the tail-flick assay. Furthermore, compound **10** produced less severe withdrawal symptoms than naloxone at high doses, and compounds **11** and **14** behaved similarly to naltrexone in the opioid-withdrawal assay. Collectively, because of the highest MOR/KOR selectivity over the DOR, the minimal MOR/DOR efficacy and low KOR efficacy in the [<sup>35</sup>S]-GTPγS binding assay, the lack of agonist property and potent MOR antagonism in the tail-flick assay, and the less severe withdrawal symptoms compared to naloxone, ligand **10** (NNP) thus represents a new lead compound to develop MOR/KOR dual-selective ligands that might possess unique therapeutic value for opioid-abuse/dependence treatment.

## EXPERIMENTAL SECTION

**Chemical Synthesis. General Methods.** Chemical reagents were purchased from either Sigma-Aldrich or Alfa Aesar. TLC analyses were carried out on Analtech Uniplate F254 plates. Chromatographic purification was accomplished on silica gel columns (230–400 mesh, Bodman). Melting points were obtained with a Fisher Scientific micro melting-point apparatus without correction. IR spectra were recorded on either a Nicolet iS10 or a Nicolet Avatar 360 FT-IR Instrument.  $^1\text{H}$  (300, 400 MHz) and  $^{13}\text{C}$  (75, 100 MHz) nuclear magnetic resonance (NMR) spectra were acquired at ambient temperature with tetramethylsilane as the internal standard on a Varian Gemini spectrometer or Bruker Ultrashield 400 Plus spectrometer, respectively. MS analysis was performed on a Quattro II triple quadrupole mass spectrometer, a Waters Micromass QTOF-II instrument (ESI source), or an Applied Bio Systems 3200 Q trap with a turbo V source for TurbolonSpray. HPLC analysis was performed with a Varian ProStar 210 system on Microsorb-MV 100-5 C18 column (250 mm  $\times$  4.6 mm) at 210/254 nm, eluting with acetonitrile (0.1% TFA)/water at 1 mL/min over 15 to 50 min. All of the above analytical methods were used to determine the purity of the newly synthesized compounds, and their purity was confirmed to be  $\geq 95\%$ .

**General Procedure 1. 14-O-Substituted Naltrexone Derivatives Synthesis.** The mixture of naltrexone (1 equiv), acyl chloride (3 equiv), and triethylamine (6 equiv) in dry DMF was heated at 100  $^\circ\text{C}$  for 6 h under  $\text{N}_2$  protection. After cooling, the reaction mixture was concentrated under vacuum to remove DMF. The resulting crude intermediate was then dissolved in MeOH and a 4%  $\text{H}_2\text{SO}_4$  aqueous solution (potassium carbonate aqueous, pH  $\approx$  10, for compounds **5** and **9**) and stirred overnight at ambient temperature. After concentration, the residue was partitioned between water and  $\text{CH}_2\text{Cl}_2$ . The water layer was extracted with  $\text{CH}_2\text{Cl}_2$  three times. The combined organic phase was then washed with brine and dried over  $\text{Na}_2\text{SO}_4$ . After removal of the solvent under reduced pressure, the resulting residue was purified using a silica gel column with a  $\text{CH}_2\text{Cl}_2/\text{MeOH}$  (150:1  $\rightarrow$  100:1) (1%  $\text{NH}_3\cdot\text{H}_2\text{O}$ ) solvent system as the eluent to give the target products **2–9** as free base.

**General Procedure 2. 14-N-Substituted Naltrexone Derivatives Synthesis with Acyl Chloride.** To a solution of 14 $\beta$ -amino-7,8-dihydro-17-cyclopropylmethyl-normorphinone (**21**, 1 equiv) in dry  $\text{CH}_2\text{Cl}_2$  was added acyl chloride (2 equiv) and  $\text{Et}_3\text{N}$  (4 equiv) on an ice-water bath under  $\text{N}_2$  protection. The mixture was then allowed to stir overnight at ambient temperature and then concentrated under reduced pressure.

**General Procedure 3. 14-N-Substituted Naltrexone Derivatives Synthesis with Acid.** On an ice-water bath, to a solution of acid (3 equiv) in anhydrous DMF (3 mL) were added *N*-(3-dimethylamino-propyl)-*N'*-ethylcarbodiimide hydrochloride (EDCI, 3 equiv), hydrobenzotriazole (HOBt, 3 equiv), 4  $\text{Å}$  molecular sieves, and TEA (5.0 equiv) under  $\text{N}_2$  protection. Fifteen minutes later, **21** (1.0 equiv) in DMF (1 mL) was added dropwise. The resultant mixture was allowed to warm to ambient temperature gradually. Upon completion of the reaction, the mixture was then filtered through Celite. The filtrate was concentrated to remove DMF.

**General Procedure 4. Saponification of 14-N-Substituted Amide Intermediates.** Methanol (5 mL) and  $\text{K}_2\text{CO}_3$  (2 equiv) were added to the residue obtained from procedure 2 or 3, and the mixture was stirred at ambient temperature overnight. The mixture was then filtered through Celite. The filtrate was concentrated to remove methanol. The residue was then partitioned between  $\text{CH}_2\text{Cl}_2$  (50 mL) and brine (50 mL). The organic layer was separated, dried over anhydrous  $\text{MgSO}_4$ , and concentrated under reduced pressure. The residue was then purified by column chromatography, eluting with  $\text{CH}_2\text{Cl}_2/\text{MeOH}$  (1%  $\text{NH}_3\cdot\text{H}_2\text{O}$ ) to afford the corresponding compound as free base.

**General Procedure 5. Hydrochloride Salt Formation.** Upon confirmation by  $^1\text{H}$  NMR, the free base was then transformed into hydrochloride salt by dissolving the base in MeOH (0.1 mL) and  $\text{CH}_2\text{Cl}_2$  (2 mL). HCl methanol solution (1.25 M, 4 equiv) was then added with an ice-water bath, and the mixture was stirred for 5 min. Diethyl ether (10 mL) was then added. Two hours later, the

precipitate was collected by filtration and dried under vacuum to give the target compound as its hydrochloride salt, which was then used for further analysis and biological assays.

**17-Cyclopropylmethyl-4,5 $\alpha$ -epoxy-3-hydroxy-14 $\beta$ -O-(pyridyl-2'-carboxy)morphinan-6-one (2).** Hydrochloride salt:  $^1\text{H}$  NMR (300 MHz,  $\text{CD}_3\text{OD}$ )  $\delta$  8.97 (m, 1H, Ar-H), 8.71 (m, 1H, Ar-H), 8.27 (m, 1H, Ar-H), 8.18 (m, 1H, Ar-H), 6.75 (d,  $J$  = 8.1 Hz, 1H, C1-H), 6.73 (d,  $J$  = 8.1 Hz, 1H, C2-H), 4.92 (s, 1H, C5-H), 4.10 (d,  $J$  = 6.6 Hz, 1H), 3.50–3.27 (m, 4H), 3.07–2.92 (m, 2H), 2.92–2.67 (m, 2H), 2.30 (m, 1H), 2.10 (m, 1H), 1.72 (m, 2H), 1.15 (m, 1H), 0.86 (m, 1H), 0.78 (m, 1H), 0.58 (m, 2H).  $^{13}\text{C}$  NMR (75 MHz,  $\text{CD}_3\text{OD}$ )  $\delta$  207.59, 161.31, 146.38, 142.36, 139.87, 138.89, 129.90, 127.39, 125.40, 119.98, 117.95, 117.50, 88.54, 61.69, 56.92, 52.99, 37.51, 34.17, 30.23, 29.30, 27.89, 26.90, 22.49, 4.97, 4.34, 1.56. MS (ESI)  $m/z$ : 447 ( $\text{M} + \text{H}$ ) $^+$ , 342. IR (KBr,  $\text{cm}^{-1}$ )  $\nu_{\text{max}}$ : 3411, 1660, 1259, 794. mp 250  $^\circ\text{C}$  (dec).

**17-Cyclopropylmethyl-4,5 $\alpha$ -epoxy-3-hydroxy-14 $\beta$ -O-(pyridyl-3'-carboxy)morphinan-6-one (3).** Free base:  $^1\text{H}$  NMR (300 MHz,  $\text{CDCl}_3$ )  $\delta$  9.57 (d,  $J$  = 1.5 Hz, 1H), 8.86 (dd,  $J$  = 1.8, 5.1 Hz, 1H), 8.45 (m, 1H), 7.52 (dd,  $J$  = 4.95, 7.95 Hz, 1H), 6.80 (d,  $J$  = 7.8 Hz, 1H), 6.66 (d,  $J$  = 8.1 Hz, 1H), 4.82 (s, 1H), 4.68 (d,  $J$  = 5.4 Hz, 1H), 3.18 (d,  $J$  = 18.3 Hz, 1H), 3.00 (m, 1H), 2.82–2.68 (m, 3H), 2.61 (dd,  $J$  = 5.85, 18.45 Hz, 1H), 2.40–2.20 (m, 4H), 1.85 (dt,  $J$  = 3.8, 14.32 Hz, 1H), 1.71 (m, 1H), 0.67 (m, 1H), 0.40 (m, 2H), 0.10 (m, 2H).  $^{13}\text{C}$  NMR (75 MHz,  $\text{CDCl}_3$ )  $\delta$  207.43, 163.37, 152.17, 149.96, 143.14, 139.31, 137.56, 137.42, 127.42, 123.75, 123.37, 119.76, 118.21, 93.97, 89.35, 58.86, 55.33, 50.85, 43.47, 35.29, 30.30, 26.56, 22.87, 9.00, 3.46, 3.30. MS (ESI)  $m/z$ : 447 ( $\text{M} + \text{H}$ ) $^+$ , 342. IR (KBr,  $\text{cm}^{-1}$ )  $\nu_{\text{max}}$ : 2946, 1716, 1282, 1108, 737. mp 202  $^\circ\text{C}$  (dec).

**17-Cyclopropylmethyl-4,5 $\alpha$ -epoxy-3-hydroxy-14 $\beta$ -O-(pyridyl-4'-carboxy)morphinan-6-one (4).** Free base:  $^1\text{H}$  NMR (300 MHz,  $\text{CDCl}_3$ )  $\delta$  8.84 (m, 2H), 8.02 (m, 2H), 6.96 (d,  $J$  = 8.1 Hz, 1H), 6.75 (d,  $J$  = 8.4 Hz, 1H), 4.73 (s, 1H), 3.24 (d,  $J$  = 6.3 Hz, 1H), 3.14 (d,  $J$  = 18.9 Hz, 1H), 3.09–2.98 (m, 2H), 2.79–2.60 (m, 3H), 2.49–2.30 (m, 4H), 2.18 (m, 1H), 1.93 (m, 1H), 0.89 (m, 1H), 0.58 (m, 2H), 0.17 (m, 2H). Hydrochloride salt:  $^{13}\text{C}$  NMR (75 MHz,  $\text{CD}_3\text{OD}$ )  $\delta$  207.27, 160.13, 147.69, 145.32, 143.50, 132.56, 129.71, 129.13, 127.53, 127.02, 123.80, 121.02, 120.88, 90.43, 70.16, 69.69, 62.11, 57.76, 49.17, 34.68, 30.97, 27.21, 23.81, 5.80, 5.23, 2.46. MS (ESI)  $m/z$ : 447 ( $\text{M} + \text{H}$ ) $^+$ , 342, 224. IR (KBr,  $\text{cm}^{-1}$ )  $\nu_{\text{max}}$ : 3385, 1755, 1724, 1270, 1241, 749. mp 190–195  $^\circ\text{C}$ .

**17-Cyclopropylmethyl-4,5 $\alpha$ -epoxy-3-hydroxy-14 $\beta$ -O-(benzoyloxy)morphinan-6-one (5).** Free base:  $^1\text{H}$  NMR (300 MHz,  $\text{CDCl}_3$ )  $\delta$  8.21 (m, 2H), 7.62 (m, 1H), 7.49 (m, 2H), 6.97 (d,  $J$  = 8.1 Hz, 1H), 6.73 (d,  $J$  = 8.4 Hz, 1H), 4.72 (s, 1H), 3.24 (m, 1H), 3.13 (d,  $J$  = 19.2 Hz, 1H), 3.10–2.95 (m, 1H), 2.80–2.60 (m, 3H), 2.50–2.40 (m, 4H), 2.34 (m, 1H), 2.18 (m, 1H), 1.90 (m, 1H), 0.89 (m, 1H), 0.58 (m, 2H), 0.17 (m, 2H). Hydrochloride salt:  $^{13}\text{C}$  NMR (75 MHz,  $\text{CD}_3\text{OD}$ )  $\delta$  205.92, 163.75, 147.54, 133.52, 132.66, 132.18, 129.39, 129.31, 123.44, 122.50, 119.74, 96.46, 93.10, 89.12, 69.35, 69.12, 62.11, 61.64, 58.04, 56.98, 33.76, 30.03, 26.89, 22.87, 4.91, 4.34, 1.56. MS (ESI)  $m/z$ : 446 ( $\text{M} + \text{H}$ ) $^+$ , 342. IR (KBr,  $\text{cm}^{-1}$ )  $\nu_{\text{max}}$ : 3398, 1730, 1239, 1055, 710. mp 161–165  $^\circ\text{C}$ .

**17-Cyclopropylmethyl-4,5 $\alpha$ -epoxy-3-hydroxy-14 $\beta$ -O-(isoquinolyl-3'-carboxy)morphinan-6-one (6).** Free base:  $^1\text{H}$  NMR (300 MHz,  $\text{CDCl}_3$ )  $\delta$  8.73 (s, 1H), 8.46 (m, 1H), 8.06 (m, 1H), 7.89 (m, 3H), 7.07 (d,  $J$  = 8.1 Hz, 1H), 6.78 (d,  $J$  = 8.1 Hz, 1H), 4.74 (s, 1H), 3.66 (d,  $J$  = 4.5 Hz, 1H), 3.27 (d,  $J$  = 5.4 Hz, 1H), 3.16 (d,  $J$  = 18.6 Hz, 1H), 2.80–2.64 (m, 2H), 2.54–2.42 (m, 2H), 2.37 (m, 1H), 2.22 (dt,  $J$  = 3.3, 12.08 Hz, 1H), 1.94 (m, 1H), 1.78–1.62 (m, 2H), 1.18 (m, 1H), 0.90 (m, 1H), 0.60 (m, 2H), 0.20 (m, 2H).  $^{13}\text{C}$  NMR (75 MHz,  $\text{CDCl}_3$ )  $\delta$  207.23, 161.70, 147.36, 138.94, 136.64, 132.23, 131.66, 130.75, 130.19, 129.85, 128.34, 128.16, 126.34, 125.01, 122.62, 119.05, 90.27, 69.63, 61.48, 58.79, 53.68, 50.25, 43.05, 33.68, 30.79, 30.38, 22.61, 8.97, 3.62, 3.45. MS (ESI)  $m/z$ : 497 ( $\text{M} + \text{H}$ ) $^+$ . IR (KBr,  $\text{cm}^{-1}$ )  $\nu_{\text{max}}$ : 3392, 2921, 1725, 1182, 781. mp 201–204  $^\circ\text{C}$ .

**17-Cyclopropylmethyl-4,5 $\alpha$ -epoxy-3-hydroxy-14 $\beta$ -O-(quinolyl-2'-carboxy)morphinan-6-one (7).** Hydrochloride salt:  $^1\text{H}$  NMR (300 MHz,  $\text{DMSO}-d_6$ )  $\delta$  9.17 (brs, 1H, exchangeable), 8.70 (d,  $J$  = 8.1 Hz, 1H), 8.27 (d,  $J$  = 8.7 Hz, 2H), 8.18 (d,  $J$  = 7.5 Hz, 1H), 7.95 (m, 1H),

7.83 (m, 1H), 7.24 (d,  $J = 8.1$  Hz, 1H), 6.94 (d,  $J = 8.7$  Hz, 1H), 5.20 (s, 1H), 4.10 (m, 1H), 3.57–3.35 (m, 2H), 3.30–3.14 (m, 2H), 3.10–2.90 (m, 2H), 2.77 (m, 1H), 2.60 (m, 1H), 2.25–2.08 (m, 2H), 1.70–1.50 (m, 2H), 1.14 (m, 1H), 0.71 (m, 1H), 0.65 (m, 1H), 0.56 (m, 1H), 0.46 (m, 1H). Free base:  $^{13}\text{C}$  NMR (75 MHz,  $\text{CDCl}_3$ )  $\delta$  209.92, 163.00, 143.76, 143.11, 140.65, 138.64, 133.72, 131.41, 130.28, 128.51, 127.38, 123.52, 122.34, 121.09, 119.50, 117.66, 115.70, 90.06, 69.90, 61.56, 58.76, 50.60, 43.20, 35.79, 30.94, 30.18, 22.20, 8.96, 3.62, 3.39. MS (ESI)  $m/z$ : 497 ( $\text{M} + \text{H}$ ) $^+$ , 342. IR (KBr,  $\text{cm}^{-1}$ )  $\nu_{\text{max}}$ : 3179, 1731, 1660, 1453, 1240, 730. mp 85–88 °C.

**17-Cyclopropylmethyl-4,5 $\alpha$ -epoxy-3-hydroxy-14 $\beta$ -O-(quinolyl-3'-carboxy)morphinan-6-one (8).** Hydrochloride salt:  $^1\text{H}$  NMR (300 MHz,  $\text{CD}_3\text{OD}$ )  $\delta$  9.64 (m, 1H, Ar-H), 9.58 (m, 1H, Ar-H), 8.40–8.17 (m, 3H, Ar-H), 7.98 (m, 1H, Ar-H), 7.27 (d,  $J = 8.1$  Hz, 1H, C1-H), 7.08 (d,  $J = 8.1$  Hz, 1H, C2-H), 5.10 (s, 1H), 4.25 (m, 1H), 3.49 (m, 2H), 3.37 (m, 2H), 3.20 (m, 1H), 3.10 (m, 1H), 2.90 (m, 1H), 2.85 (m, 1H), 2.35 (m, 1H), 2.20 (m, 1H), 2.00 (m, 1H), 1.80 (m, 1H), 1.20 (m, 1H), 0.90 (m, 1H), 0.80 (m, 1H), 0.60 (m, 2H).  $^{13}\text{C}$  NMR (75 MHz,  $\text{CD}_3\text{OD}$ )  $\delta$  206.38, 160.69, 147.10, 146.82, 144.14, 143.32, 134.82, 132.07, 129.70, 129.02, 128.44, 128.19, 127.06, 123.67, 123.29, 122.14, 120.07, 89.52, 69.37, 64.98, 61.44, 56.97, 33.87, 30.16, 26.93, 22.96, 13.57, 4.97, 4.42, 1.63. MS (ESI)  $m/z$ : 497 ( $\text{M} + \text{H}$ ) $^+$ , 342. IR (KBr,  $\text{cm}^{-1}$ )  $\nu_{\text{max}}$ : 3386, 1725, 1189, 762. mp 187 °C (dec).

**17-Cyclopropylmethyl-4,5 $\alpha$ -epoxy-3-hydroxy-14 $\beta$ -O-(2-naphthoyloxy)morphinan-6-one (9).** Hydrochloride salt:  $^1\text{H}$  NMR (300 MHz,  $\text{CD}_3\text{OD}$ )  $\delta$  8.97 (m, 1H, Ar-H), 8.10 (m, 4H, Ar-H), 7.70 (m, 2H, Ar-H), 7.21 (d,  $J = 8.1$  Hz, 1H, C1-H), 7.02 (d,  $J = 8.1$  Hz, 1H, C2-H), 4.94 (s, 1H, C5-H), 4.19 (m, 1H), 3.68 (m, 1H), 3.56 (m, 3H), 3.06 (m, 2H), 2.87 (m, 1H), 2.76 (m, 1H), 2.53 (m, 1H), 2.38 (m, 1H), 2.16 (m, 1H), 1.86 (m, 1H), 1.34 (m, 1H), 1.10–0.75 (m, 2H), 0.61 (m, 2H).  $^{13}\text{C}$  NMR (75 MHz,  $\text{CD}_3\text{OD}$ )  $\delta$  206.04, 164.81, 135.49, 132.78, 132.02, 131.25, 128.70, 128.15, 127.72, 127.36, 127.04, 126.62, 124.37, 123.53, 122.32, 121.53, 119.80, 119.17, 96.52, 93.17, 89.18, 76.69, 69.37, 61.65, 56.96, 33.79, 26.90, 22.86, 4.92, 4.39, 1.50. MS (ESI)  $m/z$ : 496 ( $\text{M} + \text{H}$ ) $^+$ , 342. IR (KBr,  $\text{cm}^{-1}$ )  $\nu_{\text{max}}$ : 3386, 1732, 1189, 1056, 776. mp 137–140 °C.

**17-Cyclopropylmethyl-4,5 $\alpha$ -epoxy-3-hydroxy-14 $\beta$ -N-[(2'-pyridyl)carboxamido]morphinan-6-one (10).** Compound 10 was prepared by following general procedures 3 and 4 in 45% yield.  $^1\text{H}$  NMR (400 MHz,  $\text{DMSO}-d_6$ )  $\delta$  9.21 (s, 1H, exchangeable), 9.19 (s, 1H, exchangeable), 8.69 (m, 1H), 8.13–8.01 (m, 2H), 7.65 (m, 1H), 6.63 (d,  $J = 8.08$  Hz, 1H), 6.60 (d,  $J = 8.12$  Hz, 1H), 4.91 (s, 1H), 3.67 (d,  $J = 5.4$  Hz, 1H), 3.04 (d,  $J = 18.4$  Hz, 1H), 2.76 (m, 1H), 2.55 (m, 2H), 2.42 (dd,  $J = 6.56, 12.72$  Hz, 1H), 2.30 (dd,  $J = 6.70, 12.66$  Hz, 1H), 2.15 (m, 1H), 2.10–1.88 (m, 3H), 1.71 (m, 1H), 1.35 (m, 1H), 0.83 (m, 1H), 0.44 (m, 2H), 0.16 (m, 2H).  $^{13}\text{C}$  NMR (100 MHz,  $\text{DMSO}-d_6$ )  $\delta$  207.26, 163.73, 149.58, 148.36, 143.36, 138.96, 138.01, 128.31, 126.70, 124.06, 121.56, 119.01, 117.29, 88.59, 58.97, 58.27, 55.85, 47.96, 43.31, 36.34, 30.01, 29.28, 21.03, 9.25, 3.75, 3.46. MS  $m/z$  found 446.3 ( $\text{M} + \text{H}$ ) $^+$ . IR (diamond,  $\text{cm}^{-1}$ )  $\nu_{\text{max}}$ : 2949, 1722, 1682, 1505, 1302, 1112. mp 195 °C (dec).

**17-Cyclopropylmethyl-4,5 $\alpha$ -epoxy-3-hydroxy-14 $\beta$ -N-[(3'-pyridyl)carboxamido]morphinan-6-one (11).** Compound 11 was prepared by following general procedures 2 and 4 in 62% yield.  $^1\text{H}$  NMR (400 MHz,  $\text{DMSO}-d_6$ )  $\delta$  9.19 (s, 1H, exchangeable), 9.03 (d,  $J = 1.64$  Hz, 1H), 8.74 (dd,  $J = 1.62, 4.78$  Hz, 1H), 8.26 (s, 1H, exchangeable), 8.17 (m, 1H), 7.55 (m, 1H), 6.60 (d,  $J = 8.08$  Hz, 1H), 6.56 (d,  $J = 8.12$  Hz, 1H), 5.00 (s, 1H), 4.06 (d,  $J = 5.4$  Hz, 1H), 2.97 (d,  $J = 18.4$  Hz, 1H), 2.71 (m, 2H), 2.47 (m, 1H), 2.44–2.23 (m, 4H), 2.11 (m, 1H), 2.04 (m, 1H), 1.56 (m, 1H), 1.32 (m, 1H), 0.78 (m, 1H), 0.39 (m, 2H), 0.08 (m, 1H), 0.04 (m, 1H).  $^{13}\text{C}$  NMR (100 MHz,  $\text{DMSO}-d_6$ )  $\delta$  208.30, 165.59, 151.61, 148.36, 143.38, 139.02, 135.26, 131.55, 128.37, 124.28, 123.44, 118.94, 117.11, 88.52, 58.86, 57.66, 57.23, 48.57, 43.14, 36.38, 29.36, 28.12, 21.42, 9.60, 3.85, 3.20. MS  $m/z$  found 446.5 ( $\text{M} + \text{H}$ ) $^+$ . IR (diamond,  $\text{cm}^{-1}$ )  $\nu_{\text{max}}$ : 2924, 1712, 1677, 1523, 1241. mp 192–195 °C.

**17-Cyclopropylmethyl-4,5 $\alpha$ -epoxy-3-hydroxy-14 $\beta$ -N-[(4'-pyridyl)carboxamido]morphinan-6-one (12).** Compound 12 was prepared by following general procedures 2 and 4 in 77% yield.  $^1\text{H}$  NMR (400

MHz,  $\text{DMSO}-d_6$ )  $\delta$  9.19 (s, 1H, exchangeable), 8.76 (d,  $J = 6.0$  Hz, 2H), 8.28 (s, 1H, exchangeable), 7.75 (d,  $J = 6.0$  Hz, 2H), 6.60 (d,  $J = 8.04$  Hz, 1H), 6.56 (d,  $J = 8.12$  Hz, 1H), 5.00 (s, 1H), 4.07 (d,  $J = 5.2$  Hz, 1H), 2.97 (d,  $J = 18.4$  Hz, 1H), 2.69 (m, 2H), 2.47 (m, 1H), 2.44–2.23 (m, 4H), 2.11 (m, 1H), 2.04 (m, 1H), 1.55 (m, 1H), 1.31 (m, 1H), 0.78 (m, 1H), 0.40 (m, 2H), 0.09 (m, 1H), 0.05 (m, 1H).  $^{13}\text{C}$  NMR (100 MHz,  $\text{DMSO}-d_6$ )  $\delta$  208.37, 165.68, 150.09 ( $\times 2$ ), 143.40, 142.98, 139.06, 128.35, 124.32, 121.59 ( $\times 2$ ), 119.04, 117.18, 88.54, 58.88, 57.79, 57.15, 48.61, 43.21, 36.39, 29.38, 28.03, 21.40, 9.62, 3.85, 3.37. MS  $m/z$  found 446.5 ( $\text{M} + \text{H}$ ) $^+$ . IR (diamond,  $\text{cm}^{-1}$ )  $\nu_{\text{max}}$ : 3270, 1710, 1686, 1604, 1510, 1221. mp 195 °C.

**17-Cyclopropylmethyl-4,5 $\alpha$ -epoxy-3-hydroxy-14 $\beta$ -N-(benzamido)morphinan-6-one (13).** Compound 13 was prepared by following general procedures 3 and 4 in 60% yield.  $^1\text{H}$  NMR (400 MHz,  $\text{DMSO}-d_6$ )  $\delta$  9.18 (s, 1H, exchangeable), 8.06 (s, 1H, exchangeable), 7.86 (m, 2H), 7.53 (m, 3H), 6.62 (d,  $J = 8.08$  Hz, 1H), 6.57 (d,  $J = 8.12$  Hz, 1H), 5.00 (s, 1H), 3.95 (d,  $J = 5.2$  Hz, 1H), 2.98 (d,  $J = 18.5$  Hz, 1H), 2.70 (m, 2H), 2.32 (m, 3H), 2.23 (m, 1H), 2.07 (m, 2H), 1.59 (m, 1H), 1.32 (m, 1H), 1.23 (m, 1H), 0.81 (m, 1H), 0.42 (m, 2H), 0.12 (m, 1H), 0.07 (m, 1H).  $^{13}\text{C}$  NMR (100 MHz,  $\text{DMSO}-d_6$ )  $\delta$  208.10, 167.23, 143.40, 138.97, 135.79, 131.09, 128.47, 128.28 ( $\times 2$ ), 127.29 ( $\times 2$ ), 124.31, 118.92, 117.14, 88.59, 58.82, 57.84, 57.04, 48.40, 43.15, 36.38, 29.53, 28.44, 21.32, 9.58, 3.83, 3.30. MS  $m/z$  found 445.3 ( $\text{M} + \text{H}$ ) $^+$ . IR (diamond,  $\text{cm}^{-1}$ )  $\nu_{\text{max}}$ : 2958, 1721, 1659, 1508, 1302, 1112. mp 180–185 °C.

**17-Cyclopropylmethyl-4,5 $\alpha$ -epoxy-3-hydroxy-14 $\beta$ -N-[(3'-isoquinolyl)carboxamido]morphinan-6-one (14).** Compound 14 was prepared by following general procedures 3 and 4 in 44% yield.  $^1\text{H}$  NMR (400 MHz,  $\text{DMSO}-d_6$ )  $\delta$  9.43 (s, 1H), 9.42 (s, 1H, exchangeable), 9.20 (s, 1H, exchangeable), 8.63 (s, 1H), 8.27 (d,  $J = 8.1$  Hz, 1H), 8.19 (d,  $J = 8.1$  Hz, 1H), 7.89 (m, 1H), 7.82 (m, 1H), 6.63 (d,  $J = 8.0$  Hz, 1H), 6.59 (d,  $J = 8.16$  Hz, 1H), 4.93 (s, 1H), 3.68 (d,  $J = 5.4$  Hz, 1H), 3.06 (d,  $J = 18.4$  Hz, 1H), 2.84 (m, 1H), 2.47 (m, 1H), 2.32 (dd,  $J = 6.78, 12.62$  Hz, 1H), 2.39 (m, 2H), 2.19 (m, 1H), 2.05 (m, 3H), 1.78 (m, 1H), 1.36 (d,  $J = 11.7$  Hz, 1H), 0.89 (m, 1H), 0.50 (m, 2H), 0.23 (m, 2H).  $^{13}\text{C}$  NMR (100 MHz,  $\text{DMSO}-d_6$ )  $\delta$  207.39, 164.26, 151.54, 143.41, 138.94, 135.39, 131.53, 129.28, 129.23, 128.42, 127.94, 127.86, 124.23, 119.62, 119.12, 117.36, 88.70, 59.19, 58.33, 55.89, 54.69, 48.01, 43.38, 36.39, 30.13, 29.46, 21.06, 9.32, 3.85, 3.53. MS  $m/z$  found 497.7 ( $\text{M} + \text{H}$ ) $^+$ . IR (diamond,  $\text{cm}^{-1}$ )  $\nu_{\text{max}}$ : 2953, 1721, 1676, 1508, 1305, 1111. mp 251–253 °C.

**17-Cyclopropylmethyl-4,5 $\alpha$ -epoxy-3-hydroxy-14 $\beta$ -N-[(2'-quinolyl)carboxamido]morphinan-6-one (15).** The title compound was prepared by following general procedures 3 and 4 in 40% yield. Hydrochloride salt:  $^1\text{H}$  NMR (400 MHz,  $\text{DMSO}-d_6$ )  $\delta$  9.23 (s, 1H, exchangeable), 9.12 (b, 1H, exchangeable), 8.65 (d,  $J = 8.6$  Hz, 1H), 8.34 (d,  $J = 8.4$  Hz, 1H), 8.21 (d,  $J = 8.5$  Hz, 1H), 8.14 (d,  $J = 8.1$  Hz, 1H), 7.94 (m, 1H), 7.78 (m, 1H), 6.79 (d,  $J = 8.1$  Hz, 1H), 6.71 (d,  $J = 8.1$  Hz, 1H), 5.57 (s, 1H), 5.49 (d,  $J = 5.8$  Hz, 1H), 3.46 (m, 2H), 3.17 (m, 2H), 2.93 (m, 1H), 2.68 (m, 4H), 2.23 (m, 1H), 1.73 (m, 1H), 1.61 (m, 1H), 1.07 (m, 1H), 0.73 (m, 1H), 0.66 (m, 1H), 0.55 (m, 1H), 0.44 (m, 1H).  $^{13}\text{C}$  NMR (100 MHz,  $\text{DMSO}-d_6$ )  $\delta$  204.73, 163.58, 147.50, 143.19, 141.16, 137.77, 135.94, 128.41, 126.94, 126.66, 126.18, 125.74, 124.35, 118.50, 117.89, 116.33, 115.92, 85.60, 55.57 ( $\times 2$ ), 54.92, 45.49 ( $\times 2$ ), 43.65, 33.12, 24.56, 19.73, 3.22, 3.09. MS  $m/z$  found 496.7 ( $\text{M} + \text{H}$ ) $^+$ . IR (diamond,  $\text{cm}^{-1}$ )  $\nu_{\text{max}}$ : 2946, 1722, 1680, 1499, 1320, 1112. mp 200–202 °C.

**17-Cyclopropylmethyl-4,5 $\alpha$ -epoxy-3-hydroxy-14 $\beta$ -N-[(3'-quinolyl)carboxamido]morphinan-6-one (16).** Compound 16 was prepared by following general procedures 3 and 4 in 48% yield.  $^1\text{H}$  NMR (400 MHz,  $\text{DMSO}-d_6$ )  $\delta$  9.29 (d,  $J = 2.12$  Hz, 1H), 9.20 (s, 1H, exchangeable), 8.82 (d,  $J = 1.84$  Hz, 1H), 8.42 (brs, 1H, exchangeable), 8.13 (m, 2H), 7.88 (m, 1H), 7.72 (m, 1H), 6.62 (d,  $J = 8.08$  Hz, 1H), 6.58 (d,  $J = 8.12$  Hz, 1H), 5.04 (s, 1H), 4.10 (d,  $J = 5.3$  Hz, 1H), 2.99 (d,  $J = 18.4$  Hz, 1H), 2.77 (m, 2H), 2.55 (m, 1H), 2.37 (m, 4H), 2.15 (m, 1H), 2.08 (m, 1H), 1.61 (m, 1H), 1.35 (m, 1H), 0.84 (m, 1H), 0.41 (m, 2H), 0.13 (m, 1H), 0.06 (m, 1H).  $^{13}\text{C}$  NMR (100 MHz,  $\text{DMSO}-d_6$ )  $\delta$  208.28, 165.62, 148.96, 148.29, 143.41, 139.04, 135.57, 131.09, 128.93, 128.66, 128.61, 128.41, 127.41, 126.46, 124.31, 118.97, 117.15, 88.57, 58.86, 57.76, 57.42, 48.61, 43.19, 36.42,

29.46, 28.22, 21.48, 9.62, 3.88, 3.25. MS  $m/z$  found 496.3 (M + H)<sup>+</sup>. IR (diamond, cm<sup>-1</sup>)  $\nu_{\max}$ : 2929, 1715, 1659, 1499, 1305, 1102. mp 185 °C.

**17-Cyclopropylmethyl-4,5 $\alpha$ -epoxy-3-hydroxy-14 $\beta$ -N-[(2'-naphthamido)morphinan-6-one (17).** The title compound was prepared by following general procedures 3 and 4 in 45% yield. <sup>1</sup>H NMR (400 MHz, DMSO-*d*<sub>6</sub>)  $\delta$  9.19 (s, 1H, exchangeable), 8.46 (s, 1H), 8.24 (s, 1H, exchangeable), 8.03 (m, 3H), 7.94 (m, 1H), 7.62 (m, 2H), 6.61 (d, *J* = 8.08 Hz, 1H), 6.57 (d, *J* = 8.12 Hz, 1H), 5.03 (s, 1H, C<sub>5</sub>-H), 4.00 (d, *J* = 5.3 Hz, 1H), 3.01 (d, *J* = 18.4 Hz, 1H), 2.73 (m, 2H), 2.56 (m, 1H), 2.34 (m, 4H), 2.09 (m, 2H), 1.63 (m, 1H), 1.35 (m, 1H), 0.83 (m, 1H), 0.43 (m, 2H), 0.16 (m, 1H), 0.09 (m, 1H). <sup>13</sup>C NMR (100 MHz, DMSO-*d*<sub>6</sub>)  $\delta$  208.05, 167.19, 143.42, 138.98, 138.0, 134.02, 133.05, 132.02, 128.64, 128.48, 127.88, 127.59, 127.52, 127.40, 126.76, 124.30, 118.92, 117.14, 88.62, 58.81, 58.00, 57.15, 48.42, 43.17, 36.41, 34.0, 28.53, 21.36, 9.61, 3.90, 3.31. MS  $m/z$  found 495.7 (M + H)<sup>+</sup>. IR (diamond, cm<sup>-1</sup>)  $\nu_{\max}$ : 3029, 1717, 1668, 1506, 1302, 1021. mp 192–195 °C.

**17-Cyclopropylmethyl-4,5 $\alpha$ -epoxy-3-hydroxy-14 $\beta$ -N-[2'-(pyridin-2'-yl)acetamido)morphinan-6-one (18).** The title compound was prepared by following general procedures 3 and 4 in 43% yield. <sup>1</sup>H NMR (400 MHz, DMSO-*d*<sub>6</sub>)  $\delta$  9.17 (s, 1H, exchangeable), 8.51 (d, *J* = 4.16 Hz, 1H), 8.10 (b, 1H, exchangeable), 7.74 (m, 1H), 7.52 (d, *J* = 7.80 Hz, 1H), 7.25 (m, 1H), 6.58 (d, *J* = 8.0 Hz, 1H), 6.53 (d, *J* = 8.0 Hz, 1H), 4.82 (s, 1H), 3.92 (s, 1H), 3.78 (m, 2H), 2.91 (d, *J* = 18.12 Hz, 1H), 2.71 (m, 1H), 2.59 (m, 1H), 2.41 (m, 1H), 2.25 (m, 4H), 2.02 (m, 2H), 1.47 (m, 1H), 1.24 (m, 1H), 0.70 (m, 1H), 0.41 (m, 2H), 0.05 (m, 2H). <sup>13</sup>C NMR (100 MHz, DMSO-*d*<sub>6</sub>)  $\delta$  208.02, 169.21, 156.41, 148.85, 143.35, 139.06, 136.60, 128.53, 124.28, 123.67, 121.80, 119.04, 117.14, 88.45, 58.90, 56.83, 56.76, 48.36, 45.79, 43.45, 36.21, 29.04, 27.86, 21.24, 9.12, 3.62, 3.47. MS  $m/z$  found 460.2 (M + H)<sup>+</sup>. IR (diamond, cm<sup>-1</sup>)  $\nu_{\max}$ : 3011, 1720, 1689, 1537, 1304, 1015. mp 195–198 °C.

**17-Cyclopropylmethyl-4,5 $\alpha$ -epoxy-3-hydroxy-14 $\beta$ -N-[3'-(pyridin-2'-yl)propanamido)morphinan-6-one (19).** The title compound was prepared by following general procedures 3 and 4 in 38% yield. <sup>1</sup>H NMR (400 MHz, DMSO-*d*<sub>6</sub>)  $\delta$  9.15 (s, 1H, exchangeable), 8.46 (m, 1H), 7.68 (m, 1H), 7.67 (s, 1H, exchangeable), 7.30 (d, *J* = 7.8 Hz, 1H), 7.19 (m, 1H), 6.56 (d, *J* = 8.1 Hz, 1H), 6.51 (d, *J* = 8.1 Hz, 1H), 4.80 (s, 1H), 3.96 (d, *J* = 5.1 Hz, 1H), 3.03 (m, 2H), 2.89 (d, *J* = 18.4 Hz, 1H), 2.68 (m, 2H), 2.55 (m, 2H), 2.38 (m, 1H), 2.20 (m, 4H), 1.96 (m, 2H), 1.41 (m, 1H), 1.18 (m, 1H), 0.76 (m, 1H), 0.42 (m, 2H), 0.09 (m, 2H). <sup>13</sup>C NMR (100 MHz, DMSO-*d*<sub>6</sub>)  $\delta$  208.44, 171.68, 160.43, 148.76, 143.34, 138.97, 136.44, 128.63, 124.46, 122.82, 121.35, 118.99, 117.03, 88.49, 58.81, 56.64, 56.58, 48.40, 43.39, 36.17, 35.32, 33.18, 28.96, 27.83, 21.25, 9.35, 3.61, 3.52. MS  $m/z$  found 474.3 (M + H)<sup>+</sup>. IR (diamond, cm<sup>-1</sup>)  $\nu_{\max}$ : 3020, 1721, 1674, 1505, 1304, 1031. mp 210–212 °C.

**17-Cyclopropylmethyl-4,5 $\alpha$ -epoxy-3-hydroxy-14 $\beta$ -N-[2'-(pyridin-2'-yl)carboxamido]acetamido)morphinan-6-one (20).** The title compound was prepared by following general procedures 3 and 4 in 37% yield. <sup>1</sup>H NMR (400 MHz, DMSO-*d*<sub>6</sub>)  $\delta$  9.15 (s, 1H, exchangeable), 9.08 (t, *J* = 5.64 Hz, 1H, exchangeable), 8.66 (m, 1H), 8.07 (m, 1H), 8.00 (m, 1H), 7.84 (s, 1H, exchangeable), 7.62 (m, 1H), 6.58 (d, *J* = 8.04 Hz, 1H), 6.51 (d, *J* = 8.08 Hz, 1H), 4.74 (s, 1H), 4.06 (d, *J* = 5.76 Hz, 2H), 3.69 (d, *J* = 5.32 Hz, 1H), 2.89 (d, *J* = 18.4 Hz, 1H), 2.71 (m, 1H), 2.52 (m, 1H), 2.46 (m, 1H), 2.16 (m, 4H), 1.97 (m, 2H), 1.55 (m, 1H), 1.23 (m, 1H), 0.53 (m, 1H), 0.27 (m, 2H), 0.02 (m, 2H). <sup>13</sup>C NMR (100 MHz, DMSO-*d*<sub>6</sub>)  $\delta$  207.64, 168.78, 164.19, 149.30, 148.52, 143.30, 138.97, 137.81, 128.54, 126.74, 124.20, 121.86, 119.04, 117.24, 88.43, 58.59, 57.58, 56.13, 48.20, 43.47, 42.95, 36.25, 29.31, 28.37, 21.06, 9.06, 3.48, 3.25. MS  $m/z$  found 503.2 (M + H)<sup>+</sup>. IR (diamond, cm<sup>-1</sup>)  $\nu_{\max}$ : 3014, 1718, 1691, 1652, 1532, 1319, 1029. mp 205–208 °C.

**Biological Evaluation. Drugs.** Morphine sulfate was purchased from Mallinckrodt (St. Louis, MO) or provided by NIDA. Morphine pellets (75 mg) and placebo pellets were provided by NIDA. Naloxone and naltrexone was purchased from Sigma-Aldrich (St. Louis, MO). All drugs and test compounds were dissolved in pyrogen-free isotonic

saline (Baxter Healthcare, Deerfield, IL) or sterile-filtered distilled/deionized water.

**Animals.** Male Swiss-Webster mice (Harlan, Indianapolis, IN) weighing 25 to 30 g were housed six per cage in animal care quarters at 22 ± 2 °C on a 12 h light/dark cycle. Food and water were available ad libitum. The mice were brought to a test room (22 ± 2 °C, 12 h light/dark cycle), marked for identification, and allowed 18 h to recover from transport and handling. Protocols and procedures were approved by the Institutional Animal Care and Use Committee at Virginia Commonwealth University Medical Center and comply with the recommendations of the International Association for the Study of Pain.

**In Vitro Competitive Radioligand Binding Assay.** The radioligand binding assay and the [<sup>35</sup>S]-GTP $\gamma$ S binding assay were conducted using monoclonal mice opioid receptor expressed in chinese hamster ovary (CHO) cell lines as described previously.<sup>38,39,44</sup> [<sup>3</sup>H]NXL, [<sup>3</sup>H]NTI, and [<sup>3</sup>H]norBNI (or [<sup>3</sup>H]DPN) were used to label the MOR, DOR, and KOR, respectively. Aliquots of a membrane protein (30  $\mu$ g) were incubated with the corresponding radioligand in the presence of different concentrations of the drug under investigation in TME buffer (50 mM Tris, 3 mM MgCl<sub>2</sub>, and 0.2 mM EGTA, pH 7.7) at 30 °C for 1.5 h. The bound radioactive ligand was separated from the free radioligand by filtration using the Brandel harvester (Biomedical Research & Development Laboratories). Specific (i.e., opioid receptor-related) binding was determined as the difference in binding obtained in the absence and presence of 5  $\mu$ M naltrexone, 5  $\mu$ M **1**, and 5  $\mu$ M 4-[(R)-[(2S,5R)-4-allyl-2,5-dimethylpiperazin-1-yl](3-methoxyphenyl)methyl]-N,N-diethylbenzamide **30** (SNC80)<sup>58</sup> for the MOR, KOR, and DOR, respectively. The potency of the drugs in displacing the specific binding of the radioligand was determined from the specific binding using linear regression analysis of Hill plots. The IC<sub>50</sub> values were then determined and corrected to K<sub>i</sub> values using the Cheng–Prusoff equation.

**In Vitro Functional Assay: Stimulation of [<sup>35</sup>S]-GTP $\gamma$ S Binding.** [<sup>35</sup>S]-GTP $\gamma$ S functional assays were conducted in the same cell membranes used for the receptor binding assays. Membrane proteins (10  $\mu$ g) were incubated with varying concentrations of drugs, GDP (10  $\mu$ M), and 0.1 nM [<sup>35</sup>S]-GTP $\gamma$ S in assay buffer (50 mM Tris, 3 mM MgCl<sub>2</sub>, 100 mM NaCl, and 0.2 mM EGTA, pH 7.7) for 1.5 h at 30 °C. Nonspecific binding was determined with 20  $\mu$ M unlabeled GTP[ $\gamma$ S]. DAMGO (3  $\mu$ M), **1** (5  $\mu$ M), and **30** (5  $\mu$ M) were included in the assay for a maximally effective concentration of a full agonist for the MOR, KOR, and DOR, respectively.

**In Vivo Pharmacology. Tail-Flick Test.** The warm-water tail-flick test was performed according to Coderre and Rollman<sup>55</sup> using a water bath with the temperature maintained at 56 ± 0.1 °C. All drugs and test compounds were administered to mice subcutaneously (s.c.). Before injecting, the baseline latency (control) of the mice was determined. Only mice with a reaction time from 2 to 4 s were used. The average baseline latency for the experiment was 3.0 ± 0.1 s. The test latency after drug treatment was assessed at the appropriate time, and a 10 s maximum cutoff time was imposed to prevent tissue damage. Antinociception was quantified according to the method of Harris and Pierson<sup>56</sup> as the percentage of maximum possible effect (% MPE), which was calculated as % MPE = [(test latency – control latency)/(10 – control latency)] × 100. The percent MPE was calculated for each mouse using at least six mice per drug.

**Opioid-Withdrawal Assay.** A 75 mg morphine pellet was implanted into the base of the neck of male Swiss Webster mice following the reported procedure.<sup>39</sup> The animals were allowed to recover in their home cages before testing. Mice were allowed to habituate for 30 min in an open-topped, square, clear Plexiglas observation chamber (26 × 26 × 26 cm<sup>3</sup>) with lines partitioning the bottom into quadrants before they were given antagonist. All drugs and test compounds were administered subcutaneously (s.c.). Withdrawal was precipitated at 72 h from pellet implantation with naloxone (1.0 mg/kg, s.c.), naltrexone (1.0 mg/kg, s.c.), and the test compounds at indicated doses. Withdrawal commenced within 1 min after antagonist administration. Escape jumps and wet dog shakes were quantified by counting their

occurrences over 20 min for each mouse using at least four mice per drug.

**Statistical Analysis.** One-way ANOVA followed by the posthoc Dunnett test were performed to assess significance using Prism 3.0 software (GraphPad Software, San Diego, CA).

**Molecular Modeling Study.** Chemical structures of the ligands were sketched in SybylX-2.0, and their Gasteiger–Hückel charges were assigned before energy minimization (10 000 iterations) with the TFF. The X-ray crystal structures for MOR (4DKL), KOR (4DJH), and DOR (4EJ4) were retrieved from the Protein Data Bank (PDB). Automated docking on these retrieved receptor structures was done utilizing genetic algorithm docking program GOLD 5.1. The binding site was defined to include all atoms within 10 Å of the  $\gamma$ -carbon atom of Asp<sup>3,32</sup> for the three opioid crystal structures along with a hydrogen-bond constraint between the 17-N of the ligand's morphinan skeleton and the carboxylate group of Asp<sup>3,32</sup>. The best CHEM-PLP scored solutions were chosen for further analyses. All molecular dynamic (MD) simulations were performed in SybylX-2.0 for 10 ps under NVT ensemble. All of the residues outside the 15 Å sphere radius of 14-C of the ligand were defined as aggregates, and MD simulations were run after assigning Gasteiger–Hückel charges and initial temperature at 300 K. The average structure of the last 1 ps of the simulation was again energy minimized after assigning Gasteiger–Hückel charges for 1000 iterations. Pictures were generated using PyMOL Molecular Graphics System, version 1.5.0.4.

## ■ ASSOCIATED CONTENT

### ● Supporting Information

Synthesis and characterization of 14-aminonaltrexone **21**, acid side chain synthesis for ligands **19** and **20**, and HPLC spectra of ligands **2–20**. This material is available free of charge via the Internet at <http://pubs.acs.org>.

## ■ AUTHOR INFORMATION

### Corresponding Author

\*Phone: 804-828-0021. Fax: 804-828-7625. E-mail: [yzhang2@vcu.edu](mailto:yzhang2@vcu.edu)

### Notes

The authors declare no competing financial interest.

## ■ ACKNOWLEDGMENTS

We are grateful to Drs. Lee-Yuan Liu-Chen (Temple University) and Ping-Yee Law (University of Minnesota) for the generous gift of opioid receptor-expressing CHO cell lines. Y.Y. and O.E. thank Irma B. Adams, Joanna C. Jacob, and Jordan O. Cox for technical guidance with the biological assays. The work was funded by a PHS grant from NIH/NIDA, DA024022 (Y.Z.). The content is solely the responsibility of the authors and does not necessarily represent the official views of the National Institute on Drug Abuse or the National Institutes of Health.

## ■ ABBREVIATIONS USED

CHO, chinese hamster ovary; DAMGO, [<sub>D</sub>-Ala<sup>2</sup>-MePhe<sup>4</sup>-Gly(ol)<sup>5</sup>]enkephalin; DOR, delta opioid receptor; DPN, diprenorphine;  $\beta$ -FNA,  $\beta$ -funaltrexamine; KOR, kappa opioid receptor; MOR, mu opioid receptor; NLX, naloxone; NTX, naltrexone; norBNI, nor-binaltorphimine; NTI, naltrindole; NAP, 17-cyclopropylmethyl-3,14 $\beta$ -dihydroxy-4,5 $\alpha$ -epoxy-6 $\beta$ -[(4'-pyridyl)carboxamido]morphinan; NAQ, 17-cyclopropylmethyl-3,14 $\beta$ -dihydroxy-4,5 $\alpha$ -epoxy-6 $\alpha$ -(isoquinoline-3-carboxamido)morphinan; TFF, TRIPOS force field

## ■ REFERENCES

- (1) Yaksh, T. L.; Wallace, M. S. Opioids, analgesia, and pain management. In *Goodman & Gilman's The Pharmacological Basis of Therapeutics*, 12th ed.; Brunton, L. L., Chabner, B. A., Knollman, B. C., Eds.; McGraw-Hill Medical: New York, 2011.
- (2) *World Drug Report 2012*; Report from the United Nations Office on Drugs and Crime: New York, June, 2012; [http://www.unodc.org/documents/data-and-analysis/WDR2012/WDR\\_2012\\_web\\_small.pdf](http://www.unodc.org/documents/data-and-analysis/WDR2012/WDR_2012_web_small.pdf).
- (3) Martin, W. R.; Eades, C. G.; Thompson, J. A.; Huppler, R. E.; Gilbert, P. E. J. The effects of morphine- and nalorphine- like drugs in the nondependent and morphine-dependent chronic spinal dog. *J. Pharmacol. Exp. Ther.* **1976**, *197*, 517–532.
- (4) Lord, J. A. H.; Waterfield, A. A.; Hughes, J.; Kosterlitz, H. W. Endogenous opioid peptides: Multiple agonists and receptors. *Nature* **1977**, *267*, 495–499.
- (5) Davis, M. P.; Pasternak, G. W. Opioid receptors and opioid pharmacodynamics. In *Opioids in Cancer Pain*, 2nd ed.; Davis, M. P., Glare, P. A., Hardy, J. R., Quigley, C., Eds.; Oxford University Press: New York, 2009.
- (6) Bart, G. Maintenance medication for opiate addiction: The foundation of recovery. *J. Addict. Dis.* **2012**, *31*, 207–225.
- (7) Veilleux, J. C.; Colvin, P. J.; Anderson, J.; York, C.; Heinz, A. J. A review of opioid dependence treatment: Pharmacological and psychosocial interventions to treat opioid addiction. *Clin. Psychol. Rev.* **2010**, *30*, 155–166.
- (8) Stotts, A. L.; Dodrill, C. L.; Kosten, T. R. Opioid dependence treatment: Options in pharmacotherapy. *Expert Opin. Pharmacother.* **2009**, *10*, 1727–1740.
- (9) Isbell, H.; Vogel, V. H. The addiction liability of methadone (amidone, dolophine, 10820) and its use in the treatment of the morphine abstinence syndrome. *Am. J. Psychiatry* **1949**, *105*, 909–914.
- (10) Walsh, S. L.; Preston, K. L.; Stitzer, M. L.; Cone, E. J.; Bigelow, G. E. Clinical pharmacology of buprenorphine: Ceiling effects at high doses. *Clin. Pharmacol. Ther.* **1994**, *55*, 569–580.
- (11) O'Brien, C. P.; Greenstein, R. A.; Mintz, J.; Woody, G. E. Clinical experience with naltrexone. *Am. J. Drug Alcohol Abuse* **1975**, *2*, 365–377.
- (12) Hollister, L. E.; Schwin, R. L.; Kasper, P. Naltrexone treatment of opiate-dependent persons. *Drug Alcohol Depend.* **1977**, *2*, 203–209.
- (13) Judson, B. A.; Carney, T. M.; Goldstein, A. Naltrexone treatment of heroin addiction: Efficacy and safety in a double-blind dosage comparison. *Drug Alcohol Depend.* **1981**, *7*, 325–346.
- (14) Minozzi, S.; Amato, L.; Vecchi, S.; Davoli, M.; Kirchmayer, U.; Verster, A. Oral naltrexone maintenance treatment for opioid dependence. *Cochrane Database Syst. Rev.* **2011**, CD001333.
- (15) Comer, S. D.; Sullivan, M. A.; Yu, E.; Rothenberg, J. L.; Kleber, H. D.; Kampman, K.; Dackis, C.; O'Brien, C. P. Injectable, sustained-release naltrexone for the treatment of opioid dependence: A randomized, placebo-controlled trial. *Arch. Gen. Psychiatry* **2006**, *63*, 210–218.
- (16) Krupitsky, E.; Nunes, E. V.; Ling, W.; Illeperuma, A.; Gastfriend, D. R.; Silverman, B. L. Injectable extended-release naltrexone for opioid dependence: a double-blind, placebo-controlled, multicentre randomized trial. *Lancet* **2011**, *377*, 1506–1513.
- (17) Broadbear, J. H.; Sumpter, T. L.; Burke, T. F.; Husbands, S. M.; Lewis, J. W.; Woods, J. H.; Traynor, J. R. Methocinnamox is a potent, long-lasting, and selective antagonist of morphine-mediated antinociception in the mouse: Comparison with clocinnamox, beta-funaltrexamine, and beta-chlornaltrexamine. *J. Pharmacol. Exp. Ther.* **2000**, *294*, 933–940.
- (18) Ward, S. J.; Portoghese, P. S.; Takemori, A. E. Pharmacological profiles of  $\beta$ -funaltrexamine ( $\beta$ -FNA) and  $\beta$ -chlornaltrexamine ( $\beta$ -CNA) on the mouse vas deferens preparation. *Eur. J. Pharmacol.* **1982**, *80*, 377–384.
- (19) Ward, S. J.; Portoghese, P. S.; Takemori, A. E. Pharmacological characterization in vivo of the novel opiate,  $\beta$ -funaltrexamine. *J. Pharmacol. Exp. Ther.* **1982**, *220*, 494–498.

- (20) Takemori, A. E.; Larson, D. L.; Portoghesi, P. S. The irreversible antagonistic properties of the fumaramate methyl ester derivative of naltrexone. *Eur. J. Pharmacol.* **1981**, *70*, 445–451.
- (21) Schmidhammer, H.; Burkard, W. P.; Eggstein-Aeppli, L.; Smith, C. F. C. Synthesis and biological evaluation of 14-alkoxymorphinans. 2. (–)-N-(Cyclopropylmethyl)-4,14-dimethoxymorphinan-6-one, a selective  $\mu$  opioid receptor antagonist. *J. Med. Chem.* **1989**, *32*, 418–421.
- (22) Spetea, M.; Schuellner, F.; Moisa, R. C.; Berzetei-Gurske, I. P.; Schraml, B.; Doerfler, C.; Aceto, M. D.; Harris, L. S.; Coop, A.; Schmidhammer, H. Synthesis and biological evaluation of 14-Alkoxymorphinans. 21. Novel 4-alkoxy and 14-phenylpropoxy derivatives of the  $\mu$  opioid receptor antagonist cyprodime. *J. Med. Chem.* **2004**, *47*, 3242–3247.
- (23) Sally, E. J.; Xu, H.; Dersch, C. M.; Hsin, L. W.; Chang, L. T.; Prisinzano, T. E.; Simpson, D. S.; Giuvelis, D.; Rice, K. C.; Jacobson, A. E.; Cheng, K.; Bilsky, E. J.; Rothman, R. B. Identification of a novel “almost neutral” micro-opioid receptor antagonist in CHO cells expressing the cloned human mu-opioid receptor. *Synapse* **2010**, *64*, 280–288.
- (24) Grimwood, S.; Lu, Y.; Schmidt, A. W.; Vanase-Frawley, M. A.; Sawant-Basak, A.; Miller, E.; McLean, S.; Freeman, J.; Wong, S.; McLaughlin, J. P.; Verhoest, P. R. Pharmacological characterization of 2-methyl-N-((2'-(pyrrolidin-1-ylsulfonyl)biphenyl-4-yl)methyl)propan-1-amine (PF-04455242), a high-affinity antagonist selective for  $\kappa$ -opioid receptors. *J. Pharmacol. Exp. Ther.* **2011**, *339*, 555–566.
- (25) Dolle, R. E.; Michaut, M.; Martinez-Teipel, B.; Seida, P. R.; Ajello, C. W.; Muller, A. L.; DeHaven, R. N.; Carroll, P. J. Nascent structure-activity relationship study of a diastereomeric series of kappa opioid receptor antagonists derived from CJ-15,208. *Bioorg. Med. Chem. Lett.* **2009**, *19*, 3647–3650.
- (26) Butelman, E. R.; Yuferov, V.; Kreek, M. J.  $\kappa$ -Opioid receptor/dynorphin system: Genetic and pharmacotherapeutic implications for addiction. *Trends Neurosci.* **2012**, *35*, 587–596.
- (27) McLaughlin, J. P.; Marton-Popovici, M.; Chavkin, C.  $\kappa$  Opioid receptor antagonism and prodynorphin gene disruption block stress-induced behavioral responses. *J. Neurosci.* **2003**, *23*, 5674–5683.
- (28) Redila, V. A.; Chavkin, C. Stress-induced reinstatement of cocaine seeking is mediated by the kappa opioid system. *Psychopharmacology* **2008**, *200*, 59–70.
- (29) Walker, B. M.; Koob, G. F. Pharmacological evidence for a motivational role of kappa-opioid systems in ethanol dependence. *Neuropsychopharmacology* **2008**, *33*, 643–652.
- (30) Xi, Z. X.; Fuller, S. A.; Stein, E. A. Dopamine release in the nucleus accumbens during heroin self-administration is modulated by kappa opioid receptors: an in vivo fast-cyclic voltammetry study. *J. Pharmacol. Exp. Ther.* **1998**, *284*, 151–161.
- (31) Tsuji, M.; Takeda, H.; Matsumiya, T.; Nagase, H.; Narita, M.; Suzuki, T. The novel kappa-opioid receptor agonist TRK-820 suppresses the rewarding and locomotor-enhancing effects of morphine in mice. *Life Sci.* **2001**, *68*, 1717–1725.
- (32) Shippenberg, T. S.; LeFevour, A.; Thompson, A. C. Sensitization to the conditioned rewarding effects of morphine and cocaine: Differential effects of the kappa-opioid receptor agonist U69593. *Eur. J. Pharmacol.* **1998**, *345*, 27–34.
- (33) Spanagel, R.; Almeida, O. F.; Bartl, C.; Shippenberg, T. S. Endogenous kappa-opioid systems in opiate withdrawal: Role in aversion and accompanying changes in mesolimbic dopamine release. *Psychopharmacology* **1994**, *115*, 121–127.
- (34) Simonin, F.; Valverde, O.; Smadja, C.; Slowe, S.; Kitchen, I.; Dierich, A.; Le Meur, M.; Roques, B. P.; Maldonado, R.; Kieffer, B. L. Disruption of the kappa-opioid receptor gene in mice enhances sensitivity to chemical visceral pain, impairs pharmacological actions of the selective kappa-agonist U-50, 488H and attenuates morphine withdrawal. *EMBO J.* **1998**, *17*, 886–897.
- (35) Kreek, M. J.; Levrán, O.; Reed, B.; Schlussman, S. D.; Zhou, Y.; Butelman, E. R. Opiate addiction and cocaine addiction: Underlying molecular neurobiology and genetics. *J. Clin. Invest.* **2012**, *122*, 3387–3393.
- (36) Wee, S.; Koob, G. F. The role of the dynorphin-kappa opioid system in the reinforcing effects of drugs of abuse. *Psychopharmacology* **2010**, *210*, 121–135.
- (37) Bruchas, M. R.; Land, B. B.; Chavkin, C. The dynorphin/kappa opioid system as a modulator of stress-induced and pro-addictive behaviors. *Brain Res.* **2010**, *1314*, 44–55.
- (38) Li, G.; Aschenbach, L. C.; Chen, J.; Cassidy, M. P.; Stevens, D. L.; Gabra, B. H.; Selley, D. E.; Dewey, W. L.; Westkaemper, R. B.; Zhang, Y. Design, synthesis, and biological evaluation of 6 $\alpha$ - and 6 $\beta$ -N-heterocyclic substituted naltrexamine derivatives as  $\mu$  opioid receptor selective antagonists. *J. Med. Chem.* **2009**, *52*, 1416–1427.
- (39) Yuan, Y.; Li, G.; He, H.; Stevens, D. L.; Kozak, P.; Scoggins, K. L.; Mitra, P.; Gerk, P. M.; Selley, D. E.; Dewey, W. L.; Zhang, Y. Characterization of 6 $\alpha$ - and 6 $\beta$ -N-heterocyclic substituted naltrexamine derivatives as novel leads to development of mu opioid receptor selective antagonists. *ACS Chem. Neurosci.* **2011**, *2*, 346–351.
- (40) Li, G.; Aschenbach, L. C. K.; He, H.; Selley, D. E.; Zhang, Y. 14-O-Heterocyclic-substituted naltrexone derivatives as non-peptide mu opioid receptor selective antagonists: Design, synthesis, and biological studies. *Bioorg. Med. Chem. Lett.* **2009**, *19*, 1825–1829.
- (41) Kourist, R.; Domínguez de María, P.; Bornscheuer, U. T. Enzymatic synthesis of optically active tertiary alcohols: Expanding the biocatalysis toolbox. *ChemBioChem.* **2008**, *9*, 491–498.
- (42) Pogorevc, M.; Faber, K. Biocatalytic resolution of sterically hindered alcohols, carboxylic acids and esters containing fully substituted chiral centers by hydrolytic enzymes. *J. Mol. Catal. B: Enzym.* **2000**, *10*, 357–376.
- (43) Zhang, Y.; Elbegdorj, O.; Yuan, Y.; Beletskaya, I. O.; Selley, D. E. Opioid receptor selectivity profile change via isosterism for 14-O-substituted naltrexone derivatives. *Bioorg. Med. Chem. Lett.* **2013**, *23*, 3719–3722.
- (44) Yuan, Y.; Elbegdorj, O.; Chen, J.; Akubathini, S. K.; Zhang, F.; Stevens, D. L.; Beletskaya, I. O.; Scoggins, K. L.; Zhang, Z.; Gerk, P. M.; Selley, D. E.; Akbarali, H. I.; Dewey, W. L.; Zhang, Y. Design, synthesis, and biological evaluation of 17-cyclopropylmethyl-3,14 $\beta$ -dihydroxy-4,5 $\alpha$ -epoxy-6 $\beta$ -[(4'-pyridyl)carboxamido]morphinan derivatives as peripheral selective  $\mu$  opioid receptor Agents. *J. Med. Chem.* **2012**, *55*, 10118–10129.
- (45) Moynihan, H.; Jales, A. R.; Greedy, B. M.; Rennison, D.; Broadbear, J. H.; Purington, L.; Traynor, J. R.; Woods, J. H.; Lewis, J. W.; Husbands, S. M. 14 $\beta$ -O-cinnamoylnaltrexone and related dihydrocodeinones are mu opioid receptor partial agonists with predominant antagonist activity. *J. Med. Chem.* **2009**, *52*, 1553–1557.
- (46) Yuan, Y.; Stevens, D. L.; Braithwaite, A.; Scoggins, K. L.; Bilsky, E. J.; Akbarali, H. I.; Dewey, W. L.; Zhang, Y. 6 $\beta$ -N-heterocyclic substituted naltrexamine derivative NAP as a potential lead to develop peripheral mu opioid receptor selective antagonists. *Bioorg. Med. Chem. Lett.* **2012**, *22*, 4731–4734.
- (47) Manglik, A.; Kruse, A. C.; Kobilka, T. S.; Thian, F. S.; Mathiesen, J. M.; Sunahara, R. K.; Pardo, L.; Weis, W. I.; Kobilka, B. K.; Granier, S. Crystal structure of the mu opioid receptor bound to a morphinan antagonist. *Nature* **2012**, *485*, 321–326.
- (48) Wu, H.; Wacker, D.; Mileni, M.; Katritch, V.; Han, G. W.; Vardy, E.; Liu, W.; Thompson, A. A.; Huang, X. P.; Carroll, F. I.; Mascarella, S. W.; Westkaemper, R. B.; Mosier, P. D.; Roth, B. L.; Cherezov, V.; Stevens, R. C. Structure of the human  $\kappa$ -opioid receptor in complex with JDTC. *Nature* **2012**, *485*, 327–332.
- (49) Granier, S.; Manglik, A.; Kruse, A. C.; Kobilka, T. S.; Thian, F. S.; Weis, W. I.; Kobilka, B. K. Structure of the  $\delta$ -opioid receptor bound to naltrindole. *Nature* **2012**, *485*, 400–404.
- (50) Bera, I.; Laskar, A.; Ghoshal, N. Exploring the structure of opioid receptors with homology modeling based on single and multiple templates and subsequent docking: A comparative study. *J. Mol. Model.* **2011**, *17*, 1207–1221.
- (51) Greiner, E.; Spetea, M.; Krassnig, R.; Schüllner, F.; Aceto, M.; Harris, L. S.; Traynor, J. R.; Woods, J. H.; Coop, A.; Schmidhammer, H. Synthesis and biological evaluation of 14-alkoxymorphinans. 18. N-Substituted 14-phenylpropyloxymorphinan-6-ones with unanticipated

agonist properties: Extending the scope of common structure-activity relationships. *J. Med. Chem.* **2003**, *46*, 1758–1763.

(52) Nieland, N. P.; Moynihan, H. A.; Carrington, S.; Broadbear, J.; Woods, J. H.; Traynor, J. R.; Husbands, S. M.; Lewis, J. W. Structural determinants of opioid activity in derivatives of 14-aminomorphinones: Effect of substitution in the aromatic ring of cinnamoylamino-morphinones and codeinones. *J. Med. Chem.* **2006**, *49*, 5333–5338.

(53) Moynihan, H.; Jales, A. R.; Greedy, B. M.; Rennison, D.; Broadbear, J. H.; Purington, L.; Traynor, J. R.; Woods, J. H.; Lewis, J. W.; Husbands, S. M. 14 $\beta$ -O-Cinnamoylnaltrexone and related dihydrocodeinones are mu opioid receptor partial agonists with predominant antagonist activity. *J. Med. Chem.* **2009**, *52*, 1553–1557.

(54) Nieland, N. P.; Rennison, D.; Broadbear, J. H.; Purington, L.; Woods, J. H.; Traynor, J. R.; Lewis, J. W.; Husbands, S. M. 14 $\beta$ -Arylpropionylamino-17-cyclopropylmethyl-7,8-dihydronormorphinones and related opioids. Further examples of pseudoirreversible mu opioid receptor antagonists. *J. Med. Chem.* **2009**, *52*, 6926–6930.

(55) Coderre, T. J.; Rollman, G. B. Naloxone hyperalgesia and stress-induced analgesia in rats. *Life Sci.* **1983**, *32*, 2139–2146.

(56) Harris, L. S.; Pierson, A. K. Some narcotic antagonists in the benzomorphan series. *J. Pharmacol. Exp. Ther.* **1964**, *143*, 141–148.

(57) Niratisai, S. Synthesis of 14 $\beta$ -amino isosteric analogs of naltrindole and norbinaltorphimine: Role of 14 $\beta$ -amino group and its acyl substituents on delta- and kappa-selective opioid receptor antagonism. Ph.D. Thesis, University of Minnesota, 2003.

(58) Calderon, S. N.; Rothman, R. B.; Porreca, F.; Flippen-Anderson, J. L.; McNutt, R. W.; Xu, H.; Smith, L. E.; Bilsky, E. J.; Davis, P.; Rice, K. C. Probes for narcotic receptor mediated phenomena. 19. Synthesis of (+)-4-[( $\alpha$ R)- $\alpha$ -((2S,5R)-4-allyl-2,5-dimethyl-1-piperazinyl)-3-methoxybenzyl]-N,N-diethylbenzamide (SNC 80): A highly selective, nonpeptide delta opioid receptor agonist. *J. Med. Chem.* **1994**, *37*, 2125–2128.